UNCLASSIFIED

CONFIDENTIAL

AD617180

WT-1117

This document consists of 56 pages

No. [illegible] of 220 copies, Series A

Operation TEAPOT

NEVADA TEST SITE

February – May 1955

Project 2.3a

NEUTRON-INDUCED RADIOACTIVE ISOTOPES IN SOILS

Classification (Cancelled) [illegible] to UNCLASSIFIED
By Authority of TASASC-3 [illegible]
By [illegible]
Issuance Date: August 7, 1958

FORMERLY RESTRICTED DATA
Handle as Restricted Data in Foreign dissemination. Section 144b, Atomic Energy Act of 1954.

This material contains information affecting the national defense of the United States within the meaning of the espionage laws, Title 18, U.S.C., Secs. 793 and 794, the transmission or revelation of which in any manner to an unauthorized person is prohibited by law.

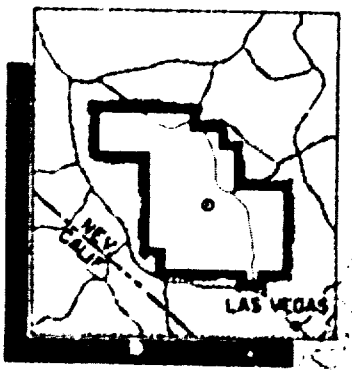

HEADQUARTERS FIELD COMMAND, ARMED FORCES SPECIAL WEAPONS PROJECT
SANDIA BASE, ALBUQUERQUE, NEW MEXICO

PROCESSING COPY
ARCHIVE COPY
EVALUATION COPY
CONFIDENTIAL
UNCLASSIFIED

WT—1117

OPERATION TEAPOT—PROJECT 2.3a

Report to the Test Director

NEUTRON-INDUCED RADIOACTIVE ISOTOPES IN SOILS

R. F. Johnson, LTJG, USN
C. S. Cook
L. A. Webb
R. L. Mather

U. S. Naval Radiological
Defense Laboratory
San Francisco 24, California

(QUALIFIED REQUESTERS MAY OBTAIN COPIES OF THIS REPORT FROM DDC.)

FORMERLY RESTRICTED DATA
[illegible] Restricted Data as defined in the Atomic Energy Act of 1954.
This material contains information affecting the National defense of the United States within the meaning of the espionage laws, Title 18, U.S.C., Secs. 793 and 794, the transmission or revelation of which in any manner to an unauthorized person is prohibited by law.
CANCELLED

SUMMARY OF SHOT DATA, OPERATION TEAPOT

Shot	Code Name	Date	Time*	Area	Type	Latitude and Longitude of Zero Point
1	Wasp	18 February	1200	T-7-4†	762-ft Air	37° 05' 11.6838" 116° 01' 18.7888"
2	Moth	28 February	0545	T-8	300-ft Tower	37° 02' 53.2854" 116° 01' 18.6867"
3	Tesla	1 March	0530	T-9b	300-ft Tower	37° 07' 31.8737" 116° 02' 51.0977"
4	Turk	7 March	0520	T-2	500-ft Tower	37° 06' 10.4944" 116° 07' 06.1179"
5	Hornet	12 March	0520	T-3a	300-ft Tower	37° 02' 25.4948" 116° 01' 31.2874"
6	Bee	22 March	0505	T-7-1a	500-ft Tower	37° 06' 41.2886" 116° 01' 28.5474"
7	ESS	23 March	1230	T-10a	67-ft Underground	37° 10' 06.1283" 116° 02' 37.7016"
8	Apple	29 March	0455	T-4	500-ft Tower	37° 06' 43.2886" 116° 06' 00.2048"
9	Wasp'	29 March	1000	T-7-4‡	740-ft Air	37° 06' 11.6838" 116° 01' 18.7888"
10	HA	6 April	1000	T-5§	36,620-ft MSL Air	37° 01' 43.2843" 116° 03' 28.7834"
11	Post	9 April	0430	T-9c	300-ft Tower	37° 07' 19.4858" 116° 02' 03.2880"
12	MET	15 April	1115	FF	400-ft Tower	36° 47' 53.6867" 116° 06' 44.1886"
13	Apple 2	5 May	0510	T-1	500-ft Tower	36° 03' 11.1886" 116° 06' 09.4827"
14	Zucchini	15 May	0500	T-7-1a	500-ft Tower	37° 06' 41.2886" 116° 01' 28.5474"

* Approximate local time, PST prior to 24 April, PDT after 24 April.
† Actual zero point 36 feet north, 426 feet west of T-7-4.
‡ Actual zero point 94 feet north, 62 feet west of T-7-4.
§ Actual zero point 36 feet south, 397 feet west of T-5.

CONFIDENTIAL

ABSTRACT

This report is concerned with that part of Project 2.3 which studied the activities induced in the surface of the earth near ground zero by neutrons released from a nuclear detonation.

Gamma-ray spectral measurements of Nevada Test Site soil obtained from the vicinity of ground zero following Shots 1, 4, and 7 have been studied. From these it is concluded that the relative quantities of observed neutron-induced activity to fission-fallout activity are functions of height, yield, and type of detonation.

Ten different soil samples were exposed to the neutrons from Shot 5. While only Na^{24} and Mn^{56} activities could be definitely found in significant quantities in all soils, the relative amounts of these two radioisotopes varied over a considerable range and, within reasonable accuracy, can be said to have been activated in proportion to the amount of sodium and manganese atoms present in the soil at the time of irradiation.

FOREWORD

This report presents the final results of one of the 56 projects comprising the Military Effects Program of Operation Teapot, which included 14 test detonations at the Nevada Test Site in 1955.

For overall Teapot military-effects information, the reader is referred to "Summary Report of the Technical Director, Military Effects Program," WT-1153, which includes the following: (1) a description of each detonation including yield, zero-point environment, type of device, ambient atmospheric conditions, etc.; (2) a discussion of project results; (3) a summary of the objectives and results of each project; and (4) a listing of project reports for the Military Effects Program.

PREFACE

The authors desire to acknowledge the assistance of, and several very profitable discussions with, M. Honma, J. Lai, and C. Callahan of the Analytical and Standards Branch, Chemical Technology Division, NRDL, with regard to the chemical analyses of the soil samples and to the problems of preparation of samples for future work.

The assistance and cooperation of W. M. Johnson, Principal Soil Correlator for the Western States, U. S. Department of Agriculture, Soil Conservation Service, in discussions concerning soil fundamentals, is gratefully acknowledged. The detailed soil description which he has supplied has been greatly appreciated.

The assistance of R. A. Taylor in electronic matters, so vital to the entire operation, cannot be adequately covered by words.

We also desire to thank Maynard Cowan of Sandia Corporation for the fine cooperation in performing this joint project.

CONFIDENTIAL

CONTENTS

CONFIDENTIAL

Chapter 1
INTRODUCTION

1.1 SCOPE OF THIS REPORT

Following a nuclear detonation, gamma radiation is observed in the vicinity of ground zero. The sources of this radiation are radioactive nuclei formed either by the fission process or by nuclear transmutations induced by neutrons. Fission products and neutron induced radioactive isotopes formed by neutron reactions in any material which is thrown into the air appear as fallout. The distribution of this fallout is dependent on the size and height of burst and the meteorological conditions at the time of burst. Radioactivity may also be induced in any other matter in the vicinity by neutrons which escape from the device.

Project 2.3, Operation Teapot, studied the spectra of both types of residual gamma radiation. This report covers those parts of the project which studied neutron induced activities exterior to the device, specifically, in this case, soils.

1.2 OBJECTIVE

The sole purpose of this report is to provide information on the nature of the gamma radiation activities induced in soils by the neutron radiations from nuclear weapons. Observations were made within the first few days after detonation. This information may serve as source material for the development of a tactically useful system for predicting similarly produced radiation from other devices over various terrain and soil configurations. However, a method for the prediction of such radiation will not be part of this report.

1.3 THEORY

1.3.1 Residual Gamma Radiation from a Nuclear Device. The residual gamma radiations which are observed following the detonation of a nuclear device are either fission product radiations or radiations from radioactive isotopes that have been produced by a neutron capture reaction. The neutron capture may occur either in material in or immediately around the device or it may occur in matter which is in the immediate vicinity of the place of detonation but which is not an intimate part of the device or associated equipment. In the latter category are the neutron capture processes which occur in the soil within a few hundred yards of ground

zero. It may also include neutron capture reactions in any equipment or other material which happens to be in the vicinity of ground zero at the time of detonation.

1.3.2 Attenuation of Neutrons-General Discussion. Neutrons which reach the soil or other material exterior to the device must first escape from the device and finally pass through the air or other matter which separates the device from the object of interest in which radioactivity is induced. During the passage through this matter, the neutrons are absorbed and scattered (attenuated) by the nuclei of this matter. These processes cause some modification in the nature, especially the energy spectral characteristics, of the neutrons.

Interactions between neutrons and other nuclear particles are of three general types: elastic scattering, inelastic scattering, and capture. Which is to be the most probable type of interaction depends on the energy of the neutron.

For fast neutrons the scattering cross section is usually considerably larger than the capture cross section. The probability of an interaction is dependent on the density of scattering nuclear particles, the density of incident neutrons, the atomic number of the scatterer, and the energy of the incident neutrons.

Neglecting certain quantum mechanical effects in which the wave length of the incident neutron must be considered, elastic scattering may be viewed as a strictly mechanical problem in which both energy and momentum must be conserved. Scattering material of low atomic number reduces fast neutrons to thermal energies much more quickly than do higher atomic number materials. For example, if a neutron traverses a medium composed of hydrogen, an average of 17.5 collisions are required to reduce a 1 Mev neutron to thermal energy. Thermal energy is considered to be about 1/40 ev. To effect the same reduction in carbon requires 111 collisions and in lead, 1800 collisions (Reference 1).

Inelastic scattering of neutrons may occur if the neutron possesses sufficient kinetic energy to raise the scattering nucleus to an excited level while being scattered. Again momentum, as well as energy, must be conserved.

If a fast neutron is captured, the resultant nucleus is always in an excited state. Often this higher state is farther above the ground state than the binding energy of one or more nuclear particles within the resultant nucleus. These nuclear particles may then escape from the nucleus. Specific reactions of this type occur when a fast neutron is captured and a proton escapes, an (n,p) reaction, or when a fast neutron is captured and an alpha particle escapes, an (n, α) reaction. Many other types of reactions may occur, depending on the energy of the incident neutron, but the two reactions mentioned are the only fast neutron reactions which appear at all possible in any quantity for nuclear device neutron energies.

Thermal neutrons are in temperature equilibrium with the surrounding nuclear material and will diffuse through this material until captured. Usually the capture of a thermal neutron adds insufficient energy to the target nucleus to allow the escape of a nuclear particle such as a proton or an alpha particle. The surplus energy available in the resultant nucleus then escapes in the form of a gamma ray, an (n, γ) reaction. Such

radiative capture reactions may also occur for incident fast neutrons but, with the exception of certain resonant energies, are much less probable for the higher energy neutrons than for thermal energies.

The probability that one of a beam of monoenergetic neutrons will pass undeviated through a target material may be expressed as an exponential function $\exp(\mu_a + \mu_s)x$, where μ_a is the absorption coefficient for the medium through which the neutron moves, μ_s is the scattering coefficient for this same medium, and x is the path length. Both the absorption coefficient and the scattering coefficient are energy dependent.

A neutron detector placed anywhere in space will be affected by all neutrons which pass through that space and which have the proper energy to be observed by that detector. Thus the detector placed at some arbitrary location in the earth, B, (illustrated in Figure 1.1) observes all neutrons passing through B. Neutrons may reach that point from the point

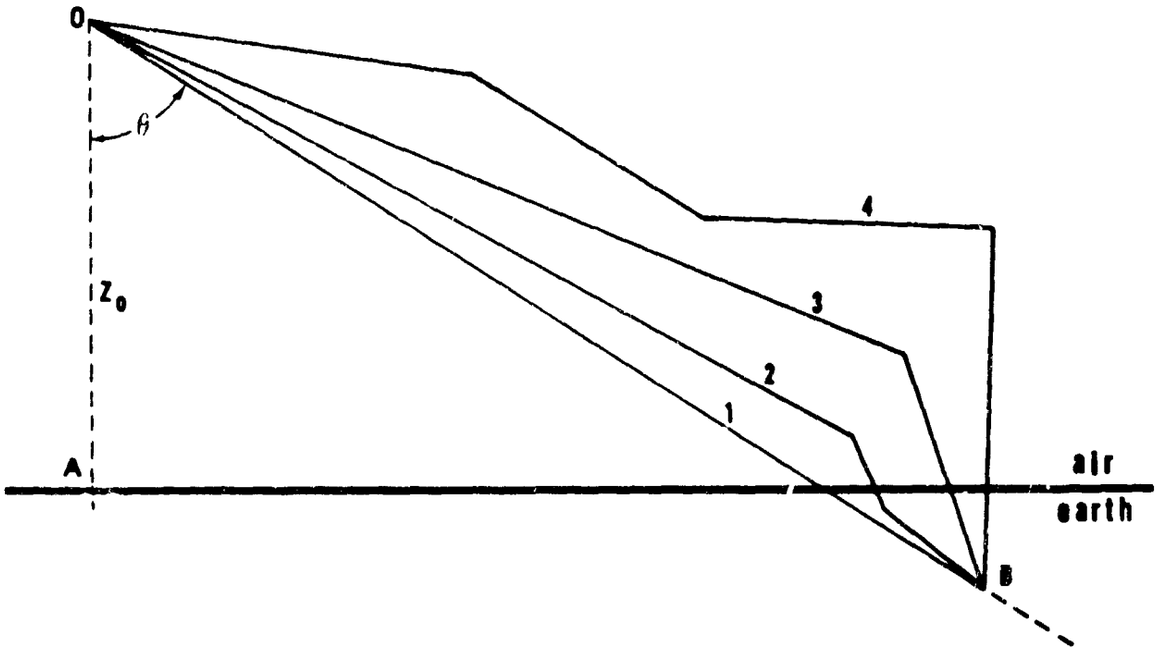

Figure 1.1 Radiation of neutrons from point of detonation.

of detonation of a device by a large number of paths such as the direct route, 1; a single scatter in the air, 3; several scatters in the air, 4; scattering in both air and soil, 2; or by many other routes which may include any number of scattering interactions. Because of this, neutrons from the device may be incident on the detector from any direction.

It is obvious that a calculation of neutron intensity cannot consider each individual scatter and capture, but must lump these into some simplified equation. The relative decrease in neutron intensity as a function of distance may be approximated mathematically through use of an effective attenuation coefficient, μ, or an effective interaction length, L, such that

$$I_2 = I_1 e^{-\mu x} = I_1 e^{-x/L}$$

Such a simple expression does not always apply since neutrons of higher

CONFIDENTIAL

energy may be scattered into a lower energy region thereby producing a buildup of lower energy neutrons. Under these circumstances this expression applies to the higher energy neutrons but not to the lower energy ones until an equilibrium situation is reached.

1.3.3 Attenuation of Device Neutrons in Air. As the neutrons radiate from the point of detonation, as illustrated in Figure 1.1, they undergo scattering interactions in the air. A measure of the rate of removal of neutrons from an arbitrarily chosen energy interval provides a first measure of the effective interaction length for that energy region. However, if there are neutrons radiated from the device having energies greater than the energy interval under consideration, a certain percentage of these higher energy neutrons will be scattered into the observed energy interval. Also, a few of the neutrons in this energy interval will be captured by appropriate nuclei in the air. At sufficient distance from the neutron source an equilibrium condition should be reached in which the number of neutrons entering a given energy interval is proportional to the number leaving. Thus the effective interaction length for all energies of neutrons will be the same at large distances from the neutron source.

Thermal neutrons are produced by the degradation of fast neutrons into the thermal energy region. Thermal neutrons are lost by capture. Therefore at sufficient distances thermal neutrons should also approach an equilibrium condition in which the effective interaction length is the same as for fast neutrons.

1.3.4 Neutron Induced Radioactive Nuclei. Radioactive isotopes are produced by all the capture processes mentioned in Section 1.3.2. The most common neutron reaction producing radioactive isotopes is the (n,γ) process; although this reaction is possible at all neutron energies, it has its largest cross section for neutrons in the thermal energy range.

It is also possible for fast neutrons to produce radioactive isotopes by other reactions such as an (n, α) or an (n,p) process, but these reactions usually have a threshold at several Mev, so are effective only within a relatively small fraction of the fission neutron spectrum. The $Fe^{56}(n,p)Mn^{56}$ reaction for example has a threshold at 2.9 Mev and its cross section reaches a peak at 14 Mev (Reference 2) of 0.11 barns. This is very small compared to the 13.3 barns for the $Mn^{55}(n,\gamma)Mn^{56}$ reaction and therefore probably does not compete significantly in the production of radioactive isotopes in soils unless very large quantities of iron are present in the soil.

1.4 PREVIOUS WORK ON SOIL INDUCED ACTIVITIES

An assessment of the problem of neutron induced activity in soil was made (Reference 3) at Operation Ranger. The five shots of this operation were detonated between 1,000 and 1,400 feet above the terrain and gave an opportunity for measuring induced soil activity without significant quantities of fallout activity. Dose rate measurements were made for each shot. Radioactive soil samples from Shot 5 were returned to USNRDL for analysis. Based on half-life measurements starting at H + 3.5 days,

the neutron induced radioactivity in the soil samples was determined to be Na^{24}. Inactive aluminum, calcium, iron, magnesium and silicon were each present in the samples to greater than 10 percent as determined by spectro-chemical analysis. Sodium and copper were determined each to be present to less than 10 percent.

Similar radiological surveys (References 4, 5, and 6) conducted at subsequent Nevada Test Site operations form the present basis for predicting neutron induced dose rates in Nevada Test Site soil. These data have been summarized in graphical form by AFSWP (Reference 7) for the prediction of gamma-ray dose rates to be expected as a result of neutron induced radioactivity in Nevada Test Site soil. Sandia Corporation has devised (References 8, 9, and 10) a system for the prediction of soil induced activity dose rates based on specific weapon models. Both the AFSWP and the Sandia Corporation work are limited to Nevada Test Site soil.

Chapter 2
PROCEDURE

2.1 SCINTILLATION SPECTROMETRY

Gamma radiation is very high energy electromagnetic radiation. It can be observed only if it interacts with matter, usually through transfer of its energy to an electron. The electron cannot retain the added kinetic energy as it passes through matter, but promptly loses it through a series of interactions with the atoms in the matter through which it moves, with the average energy loss per interaction being only a small fraction of the initial kinetic energy of the electron.

Each interaction between this electron and the matter through which the electron passes results in an excitation or ionization of an atom in the matter. When the atom returns to its normal ground state, it releases the surplus acquired energy, usually either by thermal transfer of energy to neighboring atoms or by the emission of a quantum of radiation. If the release is in the form of radiation, the energy of each quantum is much less than that of the gamma ray which initially triggered the process.

For certain transparent crystals the resulting radiation is within an easily detectable spectral region, such as the visible part of the spectrum. This phenomenon forms the basis of scintillation spectrometry. Thallium-activated sodium iodide [NaI(Tl)] is such a crystal. If the crystal makes good optical contact with a photomultiplier tube, the visible light liberates electrons photoelectrically from the photosensitive surface on the face of the tube. By applying appropriate voltage increments between successive dynodes of the photomultiplier tube, these electrons are accelerated from one dynode to the next and at each dynode secondary electron production takes place. Because of this series of electron multiplication, the final output of the tube is an electrical pulse of sufficient magnitude to produce a signal in standard, but relatively sensitive, electronic equipment. This process is illustrated in Figure 2.1. A typical crystal-photomultiplier system ready for use is shown in Figure 2.2. Because sodium iodide is deliquescent, the packaged crystal must be sealed against exposure to moisture. The crystal package has a transparent face (glass) against the photomultiplier tube, but otherwise is light tight. The photomultiplier tube is covered with black electrical tape to prevent light from leaking from the outside into the photosensitive surface of the tube. A very small leak will admit considerably larger quantities of light than is seen by the photomultiplier tube from the scintillations of the crystal.

2.2 ENERGY ABSORPTION BY A NaI(Tl) CRYSTAL

Gamma rays may interact with matter through a number of processes (Reference 11), most common of which are the photoelectric, Compton,

CONFIDENTIAL

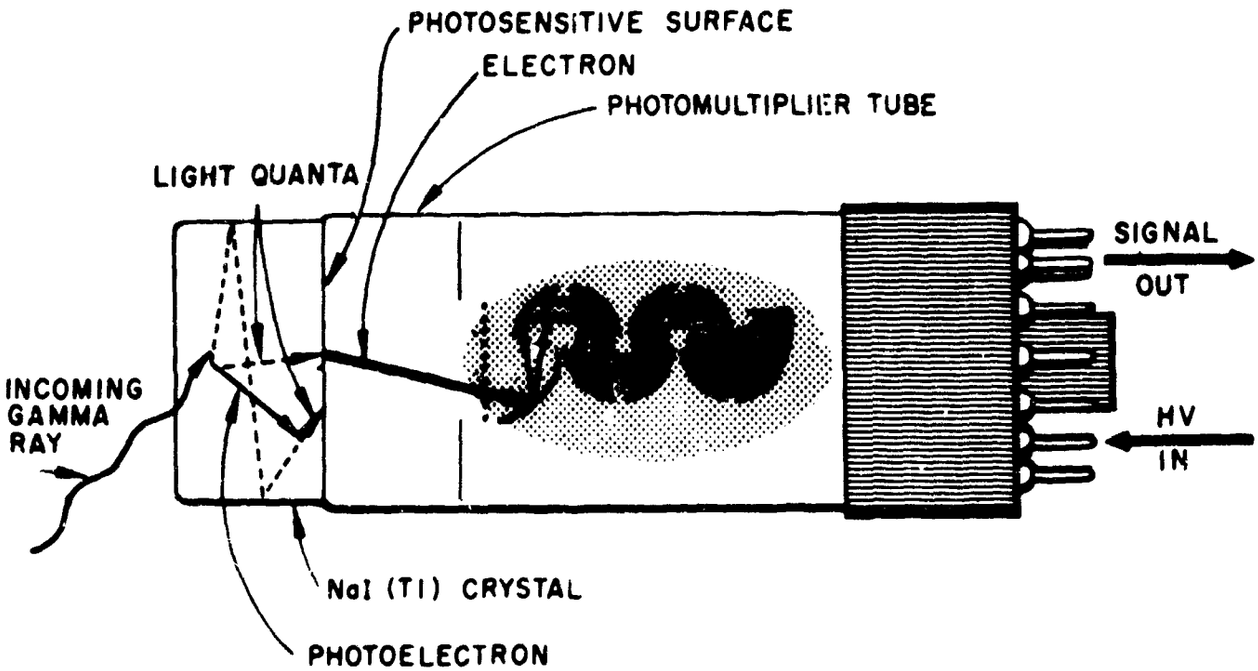

Figure 2.1 Operation of photomultiplier tube.

Figure 2.2 The 4-inch-diameter by 4-inch-high NaI(Tl) crystal and attached photomultiplier tube used for measuring pulse-height distributions from gamma radiation.

and pair production interactions. In a photoelectric interaction, the gamma quantum is completely absorbed by an atom of the crystal. Most of the energy of the gamma ray is transferred to an atomic electron, which escapes from the parent atom. In the Compton process the gamma ray is scattered by an atom in the crystal, in which case only part of the gamma-ray energy is lost and the photon continues with lower energy in a direction different from its initial direction of travel. In the pair production process the gamma quantum is also completely absorbed giving its entire energy to a pair of electrons, one positively charged (positron) and the other negatively charged (negatron) that are created at the point of interaction. Since an energy equal to the rest energy of the electron ($E = m_0c^2$) must be absorbed to create each electron of the positron-negatron pair, a gamma-ray energy of at least $2m_0c^2 = 1.022$ Mev is required before the process can take place. This process becomes significant only for gamma radiation having energies greater than several Mev. In the photoelectric effect, the photoelectron leaves the parent atom with a kinetic energy less than the energy of the incident gamma quantum, by an amount equal to the binding energy of the atomic shell from which it escapes. This kinetic energy is transformed into an electrical pulse by the crystal-photomultiplier system. The remaining gamma-ray energy is very quickly released by the parent atom when an electron from one of its outer shells falls into the shell from which the photoelectron escaped. This causes the release of one or more characteristic x-rays. Because of the relatively low energies of these characteristic x-rays, they are quickly absorbed and produce their own photoelectrons from shells having very low binding energies. Because all this happens in a time much shorter than the resolving time of the electronic equipment, all the energy appears as a single pulse, the size of which is directly proportional to the energy of the incident gamma ray.

In the Compton process the incident gamma-ray scatters from one of the electrons of the atom with which it interacts. The energies of the scattered gamma ray, and of the Compton electron, are determined as a function of the angle of scatter through use of equations derived from the laws of the conservation of momentum and energy. The Compton electron loses its kinetic energy in the crystal producing at the output of the photomultiplier tube an electrical pulse in magnitude proportional to the kinetic energy of the Compton electron. As the scattered gamma ray passes through the crystal, there is a finite probability that it, too, will undergo an interaction within the crystal. If it does, this interaction may be either a photoelectric interaction or another Compton interaction. Because of the higher photoelectric cross section for lower gamma-ray energies, the probability of this second interaction being a photoelectric process becomes greater the lower the energy of the scattered Compton gamma ray; also, the longer the path through which it must travel, the greater the probability of succeeding interactions. Because of the relatively long resolving time of the electronic equipment compared to the time required for these physical processes, the energy from any series of Compton interactions, followed by a final photoelectric interaction, will result in a single output pulse proportional to the energy of the incident gamma ray. If a Compton scattered gamma ray escapes from the crystal, the resulting electronic pulse is lower in magnitude and produces a part of a continuum of lower magnitude.

The total kinetic energy of the positron-negatron pair originating from the pair production process is 1.022 Mev less than the energy of

CONFIDENTIAL

the incident gamma ray. This produces an electronic output pulse in magnitude proportionally 1.022 Mev less than the photoelectrically produced total absorption peak of the gamma ray. However, after the positron comes to rest, it is annihilated through a merging with some negatively charged electron in the vicinity, resulting in the release of two gamma rays each with an energy $E = m_0c^2 = 0.511$ Mev. Either of these gamma rays may interact within the crystal. If the full energy of only one is absorbed (the other escaping) a pulse is developed in magnitude 0.511 Mev less than the photoelectric pulses. However, if the full energy of both quanta of annihilation radiation is absorbed, the resulting pulse is indistinguishable from a photoelectric pulse.

2.3 THE SINGLE CHANNEL GAMMA RAY SPECTROMETER

If a means is found whereby a plot may be made of the number of photomultiplier output pulses against pulse magnitude (usually called pulse height since the magnitude is seen as height on the screen of an oscilloscope), all those output pulses produced by the total absorption of the energy of individual monoenergetic gamma rays appears at the same value of pulse height and produce a peak, known as the full energy peak, in the resulting plot (References 14, 15 and 16). Gamma rays, the energy of which are not totally absorbed, form a continuous distribution between zero and the full energy peak. An electronic device capable of producing such a plot was the single channel scintillation spectrometer which was used to study the radiations from the samples returned to Mercury from the field following Shots 1, 3, 4, and 7. It consisted of an amplifier, single channel pulse height analyzer, count rate circuit, and Brown strip chart recorder, and was basically the same as had been used for similar measurements in Operation Upshot-Knothole (Reference 12) and in Operation Castle (Reference 13). The block diagram of the electronics for this apparatus is shown in Figure 2.3, and the complete spectrometer is pictured in Figure 2.4. The most significant change in the spectrometer, between the Upshot-Knothole, Castle, and Teapot measurements, has been an increase in the size of the thallium-activated sodium iodide crystal used as a detecting device for the spectrometer. For measurements in Operation Upshot-Knothole a cylindrically-shaped 1 in.-diameter by 1 in.-high crystal was used, and for Castle, a 4 in.-diameter by 4 in.-high crystal was used. For Teapot, a 7 in.-diameter by 4 in.-high crystal was used. (This crystal was loaned to this project for Teapot by the Radiation Division of the Naval Research Laboratory.) This crystal, a DuMont type 6364 photomultiplier tube, and a cathode follower preamplifier are housed in the cylindrical lead container, which sits immediately to the right of the electronic chassis. At the top of the cylindrical holder (see Figure 2.5) is a 6 in.-thick cylindrically-shaped piece of lead which acts as a shield between the crystal and a source of gamma radiation and also provides the aperture through which the radiations traverse in order to reach the crystal.

The effect of increasing the size of the crystal to enhance the total absorption effect has been shown in the Castle report (Reference 13).

CONFIDENTIAL

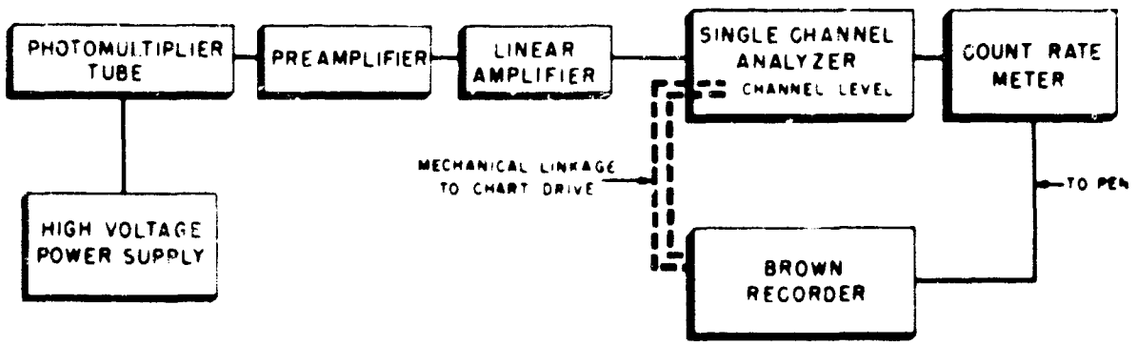

Figure 2.3 Block diagram of electronics for single-channel pulse-height analyser.

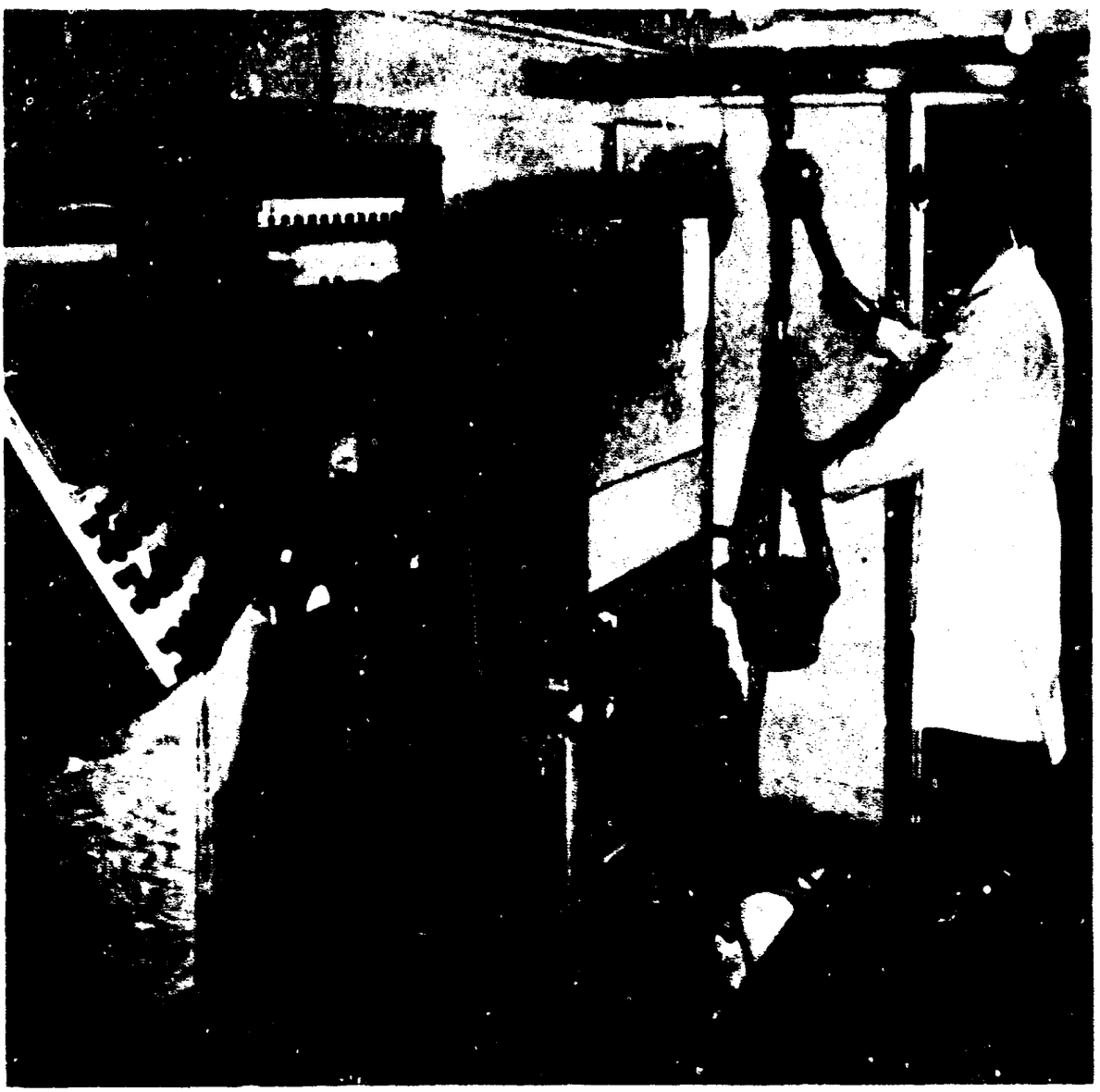

Figure 2.4 Single-channel pulse-height analyser and associated equipment in position in the Preuhauf trailer laboratory.

CONFIDENTIAL

2.4 THE TWENTY CHANNEL GAMMA RAY SPECTROMETER

Following Shot 5 the many soil samples, which had been exposed to the neutron radiation were analyzed using a 20 channel pulse height analyzer which was mounted in a 2 1/2 ton, 6 by 6, Type K53 truck. The particular mounting of this spectrometer had been made primarily for the other part of Project 2.3, the study of gamma ray radiation fields produced by fallout. However, it could still be used for the observation of gamma ray spectra emitted by individual radioactive samples. A block diagram of the electronics for this spectrometer is illustrated in Figure 2.6 and a photograph of it appears in Figure 2.7. This type of analyzer can record 20 pulse height intervals (channels) simultaneously, thereby decreasing the time required to record a spectrum. A permanent record of the information appearing on the scaling strips at the top of the spectrometer is made photographically using a modified K25 aerial photography camera mounted on the opposite wall of the truck, as illustrated

Figure 2.5 Collimator and lead shield housing the 7-inch-diameter by 4-inch-high NaI(Tl) crystal, the DuMont Type 6364 photomultiplier tube, and preamplifier.

CONFIDENTIAL

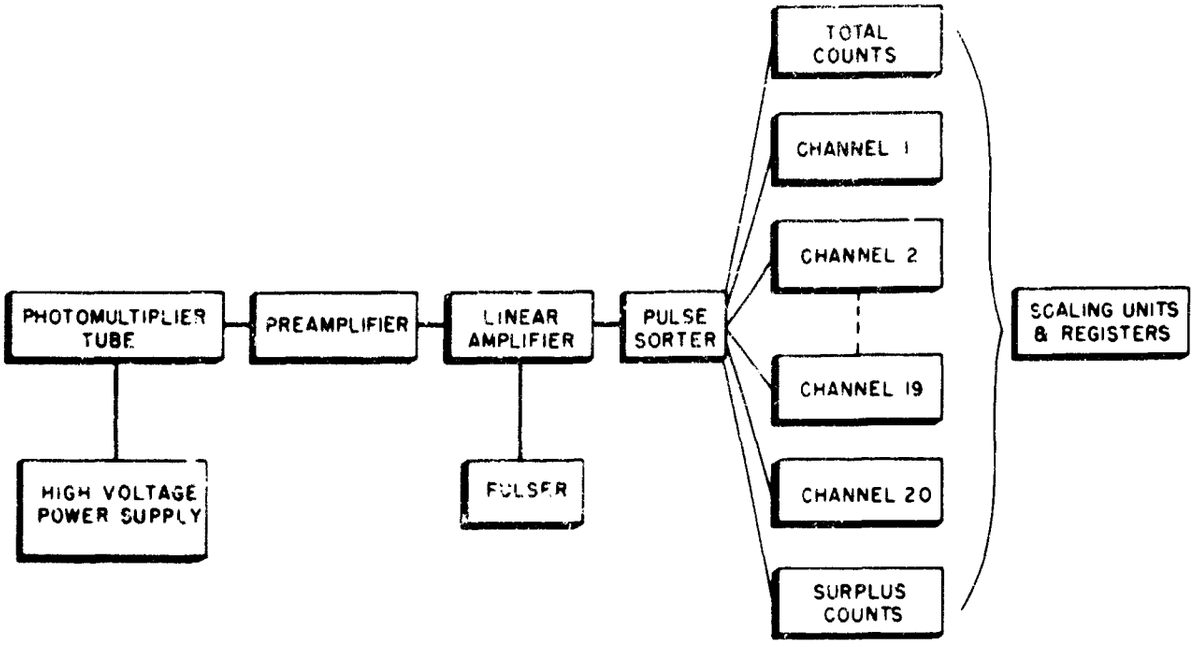

Figure 2.6 Block diagram of 20-channel gamma-ray spectrometer.

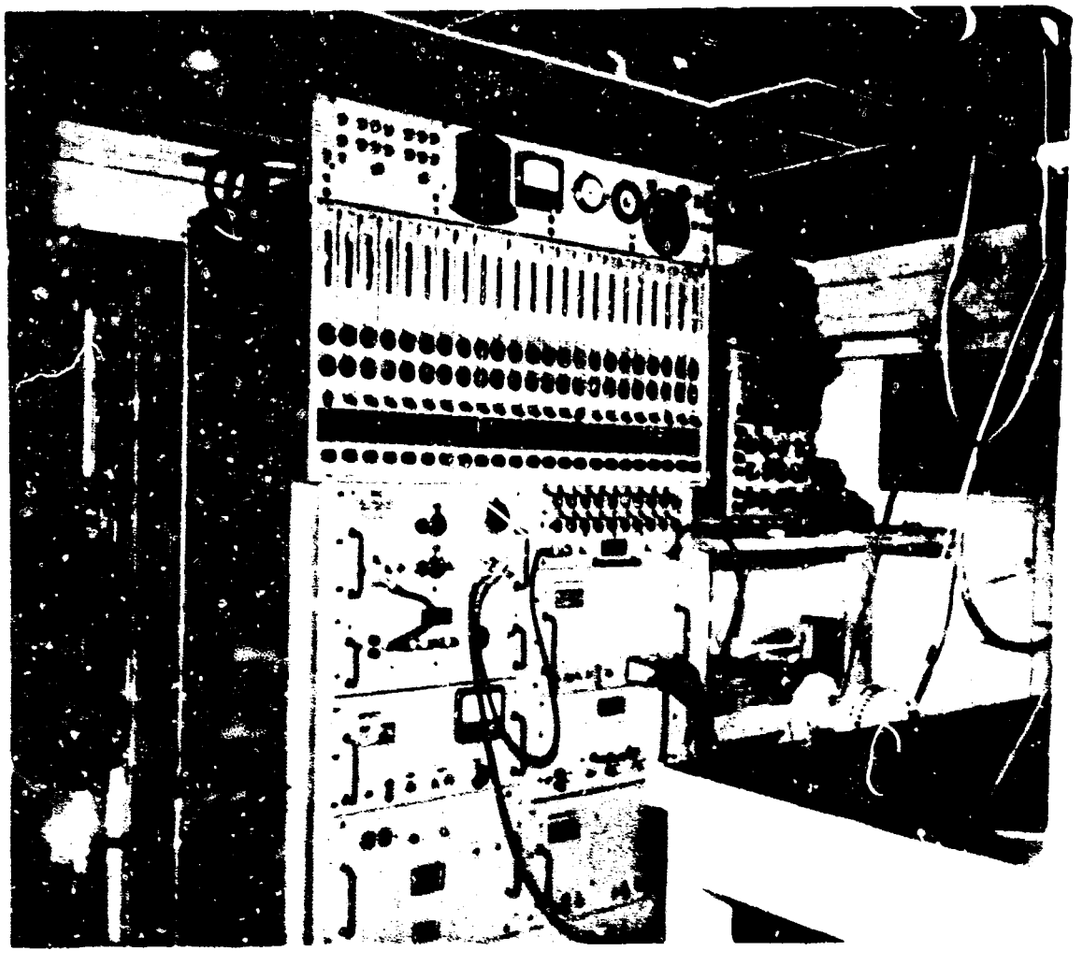

Figure 2.7 View of 20-channel gamma-ray spectrometer installed.

in Figure 2.8. These two processes permitted very rapid scanning of the samples from Shot 5, which was required because of the large number of samples and the relatively short half-lives of the isotopes present.

The detection crystal for the 20 channel analyzer consisted of a 4 in.-diameter by 4 in.-high cylindrically-shaped NaI(Tl) crystal. This crystal and associated photomultiplier and preamplifier were mounted in a lead housing 6 in.-thick on all sides and 8 in.-thick at the collimator. A cross sectional view of this system is shown in Figure 2.9.

2.5 PROCEDURE FOR SHOTS 1, 4, AND 7

Nevada Test Site soil samples were collected for Project 2.3 by several groups at the Nevada Test Site. For Shots 1, 4, and 7 these samples were simply dug from the earth in the vicinity of ground zero sometime within the first day after detonation. Their gamma-ray spectra were then analyzed on the single-channel analyzer (Reference 13) to determine qualitatively the importance of neutron induced activities.

For Shot 1 samples were obtained by a team of two men from Rad Safe who scooped up about half a shovel of dirt from the immediate vicinity of the originally planned ground zero. This was transferred to a container and returned to the laboratory at Mercury. Two samples were prepared from this soil and measured within 1 1/2 hours after the time of detonation. Similar procedures were used to obtain samples for Shots 4 and 7, using the services of personnel from Projects 2.4, 2.5.2, and 2.6.

2.6 PROCEDURE FOR SHOT 3

Several pieces of material which appeared to be of metallic nature were picked up by a Rad Safe team in the vicinity of ground zero. The spectra of these particles were followed on the single channel spectrometer for about two weeks. The radiation characteristics from these samples were those of a mixture of fission products and induced activities. Although not soil samples the fact that Na^{24} radiation was found to contribute appreciably to their total radiations, led to the inclusion of the results of the observations of their gamma radiations in this report.

2.7 PROCEDURE FOR SHOT 5

This part of Project 2.3 was conducted in cooperation with the Sandia Corporation, who, through the U. S. Department of Agriculture, procured nine representative soils for this experiment. These soils were procured from various locations within the continental limits of the United States, Hawaii, and Puerto Rico. They are considered by the U. S. Department of Agriculture as typical representatives of sands, loams, and clays. In addition, a tenth soil (Type 8) was procured at the time of Operation Teapot at the Nevada Test Site. Forty samples, four of each soil type, were prepared for exposure to neutron radiation at

Figure 2.8 Wall of K53 spectrometer truck opposite the 20-channel analyzer showing the recording camera in place.

Shot 5. The names and locations of procurement for each soil are as follows:

0.	Spring Clay Loam	Las Vegas, Nevada
1.	Conowingo Silt Loam	Pennsylvania
2.	Nipe Clay	Puerto Rico
3.	Koolau Clay	Hawaii
4.	Norfolk Fine Sandy Loam	South Carolina
5.	Carrington Loam	Iowa
6.	Chester Loam	Virginia
7.	Houston Black Clay	Texas
8.	Nevada Test Site	Area 3-A
9.	Niland Gravelly Fine Sand	Westmoreland, California

A detailed description of the soil series with which these samples are members is given in the appendix.

2.8 CHEMICAL ANALYSIS OF SAMPLES (SHOT 5)

Upon return to NRDL, a quantitative chemical analysis was performed on a portion of one sample set, 31 through 40.* The resulting iron, manganese, potassium, magnesium and sodium contents are listed in Table 2.1. This analysis was supplemented by a spectrographic analysis of samples 41 through 50, which was of a qualitative nature, and the

* The last digit of each sample number designates the soil type. Samples 11, 21, 31, and 41, for example, are the same soil, but were placed for exposure at different locations.

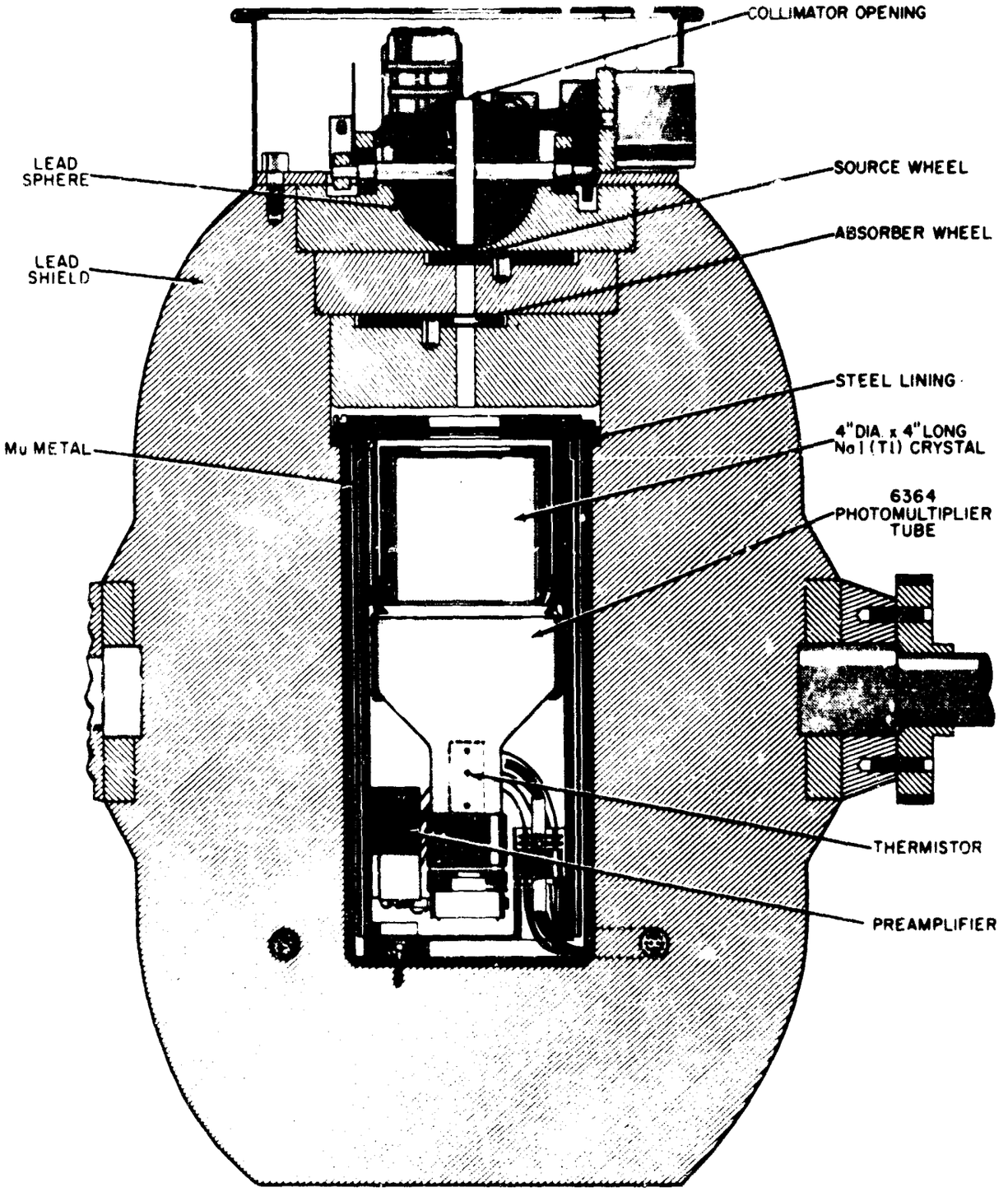

Figure 2.9 Detection crystal, photomultiplier, and preamplifier installed in lead housing.

results of which did not basically differ from the quantitative analysis. Further analysis of portions of the original U. S. Department of Agriculture (USDA) samples were made for Sandia Corporation by the Smith-Emery Company of Los Angeles. Their results are listed in Table 2.2.

For some samples there is a decided variation between the soil chemical composition reported by the two groups. This variation appears to be real and is apparently caused by lack of homogeneity in the original sample material. Upon visual examination of any soil, it is immediately apparent that the various constituents in the soil are not uniformly mixed. Since the samples analyzed for Sandia Corporation were taken from the initial material (approximately 12 pounds) delivered by USDA and the NRDL analyses were made on the small test tube samples (approximately 5 grams) whose radiation had been studied with the scintillation spectrometer, it is not surprising that differences in chemical composition may occur. Thorough mixing, as for example ball milling, of each of the soils before exposure or chemical analysis would have given a truer picture of the soils' average chemical composition and would have achieved greater uniformity between samples of the same series in this experiment.

2.9 EXPOSURE PROCEDURE AT SHOT 5

For exposure to the neutron flux each sample was contained in a short-length of 1 1/2 inch iron pipe, capped at both ends as shown in Figure 2.10. In all, forty samples were attached to a cable* which ran radially from ground zero to an anchor point outside the expected radiation fields. The distribution of the samples on this cable was as follows:

Samples 11 - 20	50 yards from GZ
Samples 21 - 30	150 yards from GZ
Samples 31 - 40	250 yards from GZ
Samples 41 - 50	350 yards from GZ

A bracket was welded on each container and used to bolt the pipe to the cable.

2.10 COLLECTION AND PREPARATION OF SPECTROMETER SOURCES (SHOT 5)

At approximately H + 3 hr all forty samples were brought, immediately after recovery and in their exposure containers, to the Control Point at the Nevada Test Site. There, enough material was taken from each container to fill a test tube of approximately 3/8 inch diameter to a depth of 2 to 2 1/2 inches. Equal volumes of each sample, as near as could be determined visually, were used. All samples were numbered from the original exposure container to eliminate any possible errors in transfer.

---

* By M. Cowan, Sandia Corporation

CONFIDENTIAL

TABLE 2.1 ANALYSIS AT NRDL IN PERCENT BY WEIGHT

Sample No.	Fe_2O_3	MnO	MgO	K	Na
J	0.75	0.0122	5.05	0.63	1.50
1	3.92	0.211	--	1.60	0.51
2	54.0	0.271	0.23	0.05	0.06
3	34.2	0.0377	0.35	0.46	0.22
4	0.79	0.00796	0.03	0.08	0.04
5	2.75	0.0847	0.54	1.11	0.77
6	3.31	0.0341	0.50	1.43	0.28
7	2.74	0.0458	2.45	0.52	0.08
8	1.25	0.0687	1.04	2.53	1.51
9	3.91	0.100	1.98	1.77	3.25

TABLE 2.2 ANALYSIS BY SCOTT-MONEY COMPANY IN PERCENT BY WEIGHT

Sample No.	Mn	Na	K
0	0.020	1.30	0.51
1	0.160	0.27	1.36
2	0.240	0.06	0.07
3	0.067	0.0[illegible]	0.38
4	0.022	less than .01	0.05
5	0.070	0.50	1.03
6	0.036	0.19	1.59
7	0.059	0.06	0.50
8	0.059	1.63	2.91
9	0.084	2.70	1.64

CONFIDENTIAL

2.11 PROCEDURE FOR TAKING DATA FOLLOWING SHOT 5

For analysis, each sample was placed in identical geometry relative to the lead collimator and crystal. The bottom of each test tube was 2 1/2 inches above the top of the 1/2 inch diameter aperture in the lead collimator. Thus, as seen by the crystal, each sample was in consistently good geometry.

The pulse height distribution of each sample was observed from 0 to 4 Mev over forty channels and from 0 to 300 kev over twenty channels

Figure 2.10 Sample exposure, Shot 5.

in the initial runs. It became immediately apparent that there was no information of value in the lower energy region and these measurements were discontinued in later runs.

Background pulse-height distributions were taken at intervals during the sample runs. In all cases the background was negligible relative to the sample counting rate.

Pulse-height distributions were observed a second time from 12 to 24 hours after the initial data were recorded. The later pulse height distributions for samples 21, 22, 27, and 28 were used to verify the results from the earlier analyses. Agreement in all but one case was good, and well within the experimental errors.

CONFIDENTIAL

Chapter 3
DATA REDUCTION

3.1 ANALYSIS OF PULSE-HEIGHT SPECTRA FROM SHOT 5

From the observed data, pulse-height spectra, without correction or normalization, were prepared. A typical example is illustrated in Curve A of Figure 3.1 for Sample 18.

The center of the 2.76 Mev full energy peak of Na^{24} was used as the energy scale calibration mark. The peak was apparent in all but a few cases and in those samples where the 2.76 Mev peak could not be seen the 0.845 Mev full energy peak of Mn^{56} was used as the calibration peak. The center of the Na^{24} peak was located by assuming it to have Gaussian form. This center of the Gaussian was normalized to fall in the twenty-eighth channel. Under these conditions, the 0.845 Mev peak of Mn^{56} was located in the eighth channel, since the first channel did not begin at zero but at approximately 100 kev.

The process of normalization was the progressive broadening of each channel. This compressed the total raw pulse-height spectrum into a smaller number of channels, placing the center of the individual total absorption peaks at a normalized position on the energy scale (Curve B of Figure 3.1). At least a portion of this normalization is required to compensate for a shift in gain due to the temperature fluctuations of the crystal and a shift of gain within the amplifiers of the analyzer.

As a result of the above manipulation, direct comparison could be made between spectra, since each spectrum could now be analyzed in an identical manner. The full energy peak area was used as the basis for this analysis. The channel in which a full energy peak is observed includes background counts (usually so small as to be insignificant) and counts from the Compton distributions of higher energy peaks. To find the true area of each superimposed peak, it was necessary to unfold the spectra, which means that the Compton distributions for higher energy peaks were successively subtracted from the normalized pulse height distribution. In this way, a series of full energy peaks and their associated Compton distributions were evolved, as illustrated in Curve B of Figure 3.1. The pulse height distributions of five different gamma rays can be seen in Figure 3.1. The highest energy peak belongs to the 2.76 Mev gamma ray of Na^{24}. The shaded area 5 is the Compton distribution associated with this peak. This Compton distribution must be subtracted from the rest of the spectrum to determine magnitude and location of the full energy peak of next lowest energy. This peak belongs to the 2.1 Mev gamma ray of Mn^{56} for which the solidly-shaded area 4 is the Compton distribution. Subtraction of this area leaves the 1.8 Mev gamma ray full energy peak of Mn^{56} as the next lowest energy gamma ray, for which the shaded area 3 is the Compton distribution. Similar analysis shows that the shaded areas 1 and 2 are respectively the Compton distri-

CONFIDENTIAL

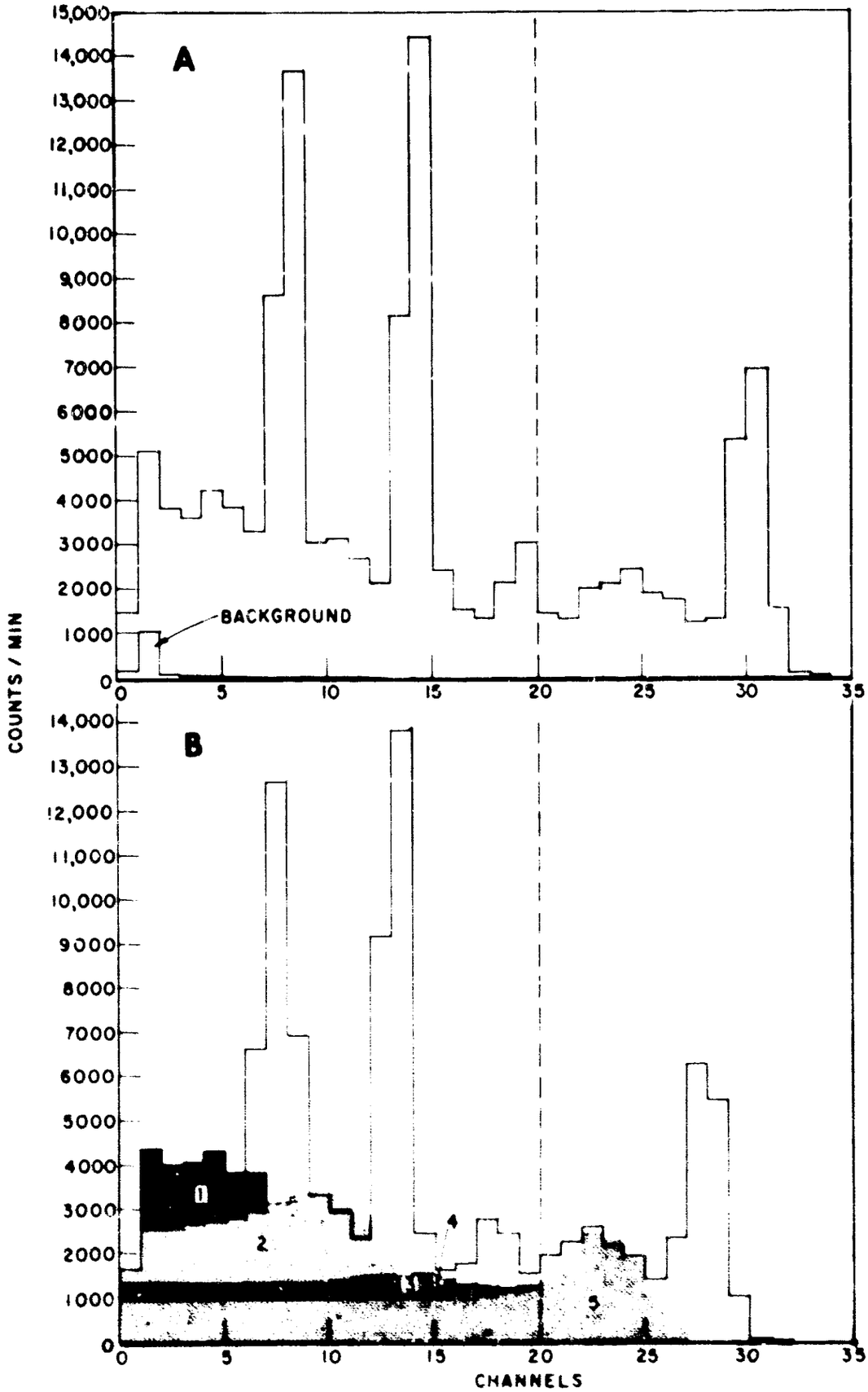

Figure 3.1 Pulse-height spectra. A, without correction or normalization; B, normalized (see Section 3.1).

CONFIDENTIAL

butions for the 0.845 Mev gamma ray of Mn^{56} and the 1.38 Mev gamma ray of Na^{24}.

The unfolding system, from which the shape and area of the Compton distributions were determined relative to the area of the full energy peaks for the particular NaI(Tl) crystal used in these experiments was derived from the Compton distributions of five known gamma ray sources (Hg^{203}, Na^{22}, Mn^{56}, K^{42}, and Na^{24}) and the Berger-Dogget (Reference 14) theoretical Compton distributions. The results of this derivation was a specific peak-to-total function for the NaI(Tl) crystal used in this set of experiments.

In addition to the peak-to-total correction used to determine the total number of gamma-quanta observed by the crystal, a second correction was required to add those gamma rays which traverse the crystal without undergoing a Compton, photoelectric or pair production interaction. This correction has been calculated and is sometimes called the $(1-e^{-\mu x})$ correction, since this equation, with μ being the total absorption coefficient of NaI, gives the relative number of gamma-quanta which traverse the crystal with no interaction.

A third correction was required to account for the porosity of the lead collimator to gamma radiation. The apparent transmission through the edges of the lead collimator has been calculated and found to be significant for gamma-ray energies above 400 kev. This porosity has been confirmed experimentally and appropriate corrections have been made in the calculations. The porosity correction factor as a function of gamma-ray energy is shown in Figure 3.2.

After these three corrections have been applied, the number of gamma rays of each energy entering the NaI(Tl) crystal through the aperture of the collimator will have been determined.

At the energies involved, the self-absorption effects of the source material and of the air between source and detector were negligible.

3.2 CALCULATION OF NUMBER OF Na^{24} AND Mn^{56} ATOMS AT TIME ZERO

To determine the number of radioactive atoms at time zero, three additional corrections were required.

The first was a correction to time zero from the time of observation of the rate of emission of gamma radiation. Since the radiations of only two radioactive isotopes, Na^{24} and Mn^{56}, were found, the adjustment could be made relatively easily, using the known decay constants of these two isotopes.

The second correction determined the number of radioactive atoms needed at time zero to produce the rate of emission observed in the crystal. This was derived from the equation, $dN/dt = \lambda N$.

Since the emission observed by the crystal was that from only a small fraction of 4π steradians, a solid angle correction was also required. This was determined by calculation from the known geometry of the experiment and was calculated to be (1.197×10^{-4}) of 4π steradians. A final correction, dividing by the weight of the sample, was required to determine the number of radioactive atoms per gram of soil. The samples were prepared to have as near equal volume as possible. However,

CONFIDENTIAL

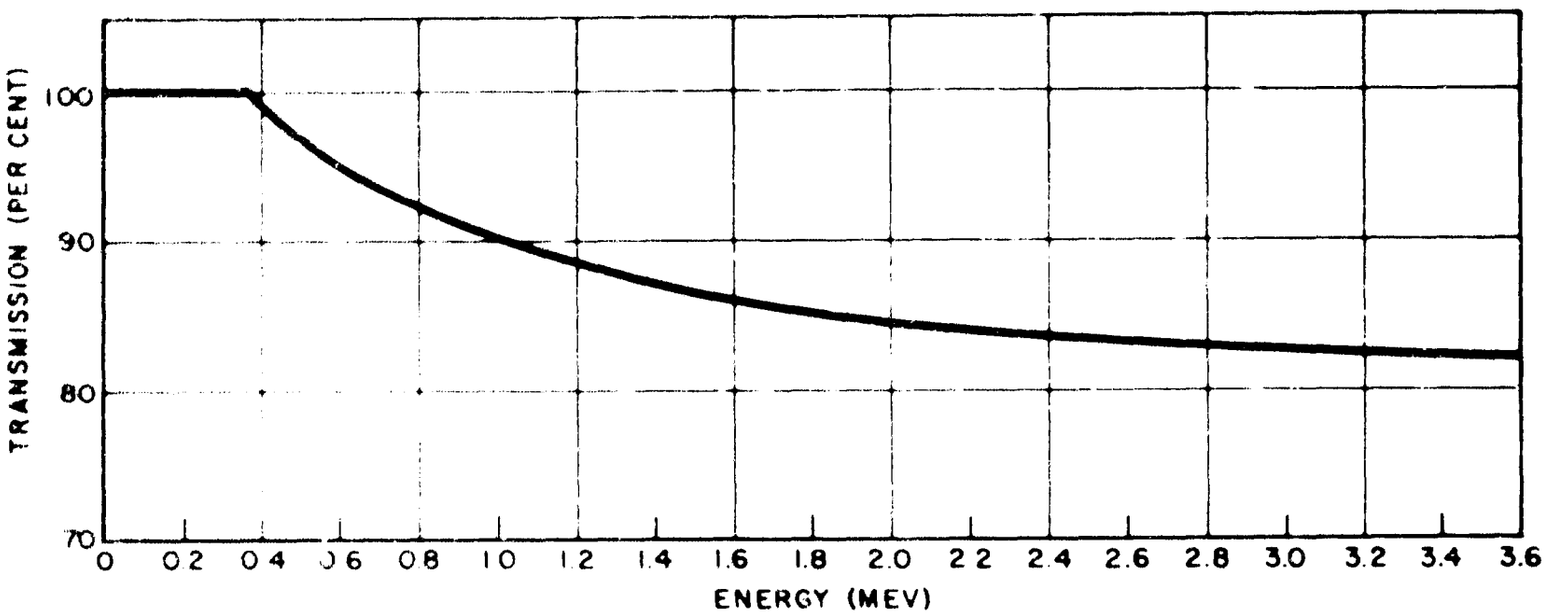

Figure 3.2 Porosity correction factor as a function of gamma-ray energy.

their densities did vary considerably, such that the increment of weight between different samples was relatively large, percentage-wise.

A final formulation may now be given for the number, N, of activated atoms at the time of detonation of the device of each individual type in each soil sample per unit weight of soil sample. This formula is

$$N \equiv \frac{(dN/dt)(KA)}{(e^{-\lambda t})(W)(KB)(1 - e^{-\mu x})(\lambda)(KC)}$$

where dN/dt is the measured count rate
KA is the porosity correction factor
$e^{-\lambda t}$ is the zero time correction (to time of detonation)
W is weight of sample
KB is the peak to total correction
$(1 - e^{-\mu x})$ is the crystal interaction correction
λ is the decay constant
KC is the geometrical correction

3.3 ESTIMATED MAGNITUDE OF ERRORS

Each of the specific manipulations in the system of analysis just described has an associated error. An estimate of these errors is as follows:

1. Determination of the total number of counts in the pulse height distribution relative to the number in the full energy peak (peak to total correction) as a function of energy for the specific crystal used in this experiment. Estimated error is $\pm$1 percent.

2. Determination of the number of gamma rays which traverse the crystal without interaction $(1 - e^{-\mu x})$ correction as a function of energy. Estimated error $\pm$2 percent.

3. Geometric correction to determine the solid angle subtended by the crystal. Estimated error $\pm$2 percent.

4. Porosity (transmission) correction as a function of energy for the number of gamma rays transmitted through the edges of the lead collimator. Estimated error $\pm$5 percent.

5. The decay constant correction, λ, for Na^{24} and Mn^{56}. Estimated error $\pm$1 percent.

6. There is also a general statistical counting error taken as $\pm\sqrt{N_o}$ where N_o represents the gross raw photons counted within each photopeak.

7. The zero time correction was known within an estimated error of $\pm$0.1 percent. This error was insignificantly small and therefore was not considered in the results.

8. The weight of each sample was known within an estimated error of $\pm$0.1 percent. This error was insignificantly small and therefore was not considered in the results.

Inherent within the system of Compton subtraction is a systematic error. This error evolves from the formulation of the subtraction curves and the reading accuracy of the graphs. This error, plus other small systematic errors, are estimated as probably not more than $\pm$5 percent, and this error has been added to the random probable errors.

CONFIDENTIAL

Chapter 4
RESULTS and CONCLUSIONS

4.1 RESULTS AND CONCLUSIONS FOR SHOTS 1, 3, 4, AND 7

Preliminary exploratory measurements using the single-channel analyzer were made of samples picked up from the first shots of the Teapot series from which it was apparent that induced activities were major contributors to some of the sample activities. These activities were identified in the field as Na^{24} and Mn^{56} by gamma-ray energy and half life. Later examination of other data revealed that K^{42} is also a possible contributor but its gamma-ray energy and half life can be easily masked by that of Na^{24} and its contribution is relatively small.

Spectral measurements were made on ground samples from Shot 1 (750 ft air burst), from Shot 4 (500 ft tower shot), and from Shot 7 (underground shot), which show respectively: pure induced activities, mixed fission-product and induced activities, and almost pure fission-product activities (for this discussion the induced activities from bomb components, especially Np^{239}, are lumped with the fission-product activities, since they are intimately mixed together in the explosion). Also reported are the spectra from the metallic samples picked up at Shot 3 (300 ft tower shot).

The spectra from Samples 1-1 and 1-2* are shown in Table 4.1. Samples were obtained by a team of two men from Rad Safe who scooped up about half a shovel of dirt from the immediate vicinity of the originally planned ground zero. This was transferred to a container and returned to the laboratory at Mercury. Samples 1-1 and 1-2 were both prepared from this soil. The test tube was filled to a depth of 3/8 inch for Sample 1-1 and to a depth of one inch for Sample 1-2. The assignment of gamma-ray activities was checked by exposing samples of NaCl and Fe (probably containing some Mn) to the neutrons from Shot 2. The 0.5 Mev line which appears along with those of the induced activities could be annihilation radiation from an induced-positron activity or from pair production by high-energy radiation, such as the 2.8 Mev line from Na^{24}. Relative to the amount of Na^{24}, the amount of Mn^{56} in Sample 1-1 is only 56 percent of that in Sample 1-2 (after decay corrections). This is indicative of the sampling errors involved in this sort of measurement.

The spectra from Sample 3-2, a metallic piece, gathered near ground zero is shown in Table 4.1 and has both fission product and induced activity lines. The 1.4 Mev line attributed to Na^{24} appears to have excess intensity in the first spectra and may indicate the presence of another activity.

---

* In numbering samples, the first number designates the shot, the second number the particular sample.

CONFIDENTIAL

The spectra from Samples 4-1 (taken by Project 2.6 personnel at 2,400 yards South from ground zero) and 4-3 (taken by Project 2.4 personnel at 600 yards East from ground zero) are also shown in Table 4.1. The samples were gathered in a manner similar to Samples 1-1 and 1-2. The discrepancy in the data of Sample 4-1 raises some question of the assignment of the line to the Na^{24} activity because the 2.75 line is absent in the first 3/8/55 spectra and the 1.38 (?) line has disappeared in the 3/8/55 spectra (20 hours later); whereas it should still be visible if the half life were 14 hours as for Na^{24}. It is possible that errors could have been made in the data recording process, but there is no method of checking now. It is possible that the activity is not Na^{24} in this sample, but there is insufficient information to reach this conclusion. The intensity of the two Na^{24} lines should be equal. The excess of intensity in the 1.4 line might be due to the 1.5 line of K^{42} (in Sample 4-3, for example).

For comparison, a spectra taken at a comparable time from Sample 7-1 is included in Table 4.1, in which no gamma lines ascribable to Na^{24} can be detected.

These data appear to be consistent with the following picture: the total fission-product activities are overwhelmingly greater than the total activities induced in nearby soil material by the neutrons from the device. For devices which are exploded at a height of several fireball radii, such as Shot 1, the fission products are carried away in the fallout cloud, but activities are induced in the soil near ground zero, and soil samples taken near ground zero show essentially only soil induced activities. For lower altitude shots, such as a tower shot (Shots 3 and 4) for which some of the soil found near ground zero has been carried into the stem and cloud produced by the device, a more-equal ratio of soil induced activities relative to fission product activities is found, while samples obtained at greater distances from ground zero show decreasing amounts of induced activities relative to fission product activities. In the case of a surface or underground shot, such as Shot 7, for which the soil induced activities are thoroughly mixed with the weapon debris, the whole of the resulting mixture is distributed as fallout. The soil induced activities will be small (not more than a few percent) everywhere compared to the fission product activities.

This has important consequences for these special cases. The decay rate of the induced soil activity is a mixture of exponential decays due to the 2.59-hour half life of Mn^{56} and the 15.0-hour half life of Na^{24} instead of the $t^{-1.2}$ decay typical of fission products. The gamma spectrum contains a large amount of the highly penetrating 2.75 Mev gamma line from Na^{24}, while the effective upper limit of the fission-product gamma spectrum is 1.6 Mev.

4.2 RESULTS FROM SHOT 5

The results from each sample, 11 - 50, are shown in Table 4.2. Columns A and B respectively give the number of atoms of Na^{24} and Mn^{56} at zero time per gram of soil, as calculated in accordance with the procedures described in paragraphs 3.1 and 3.2. Column C is the ratio of Mn^{56} to Na^{24} at time zero for each sample.

TABLE 4.1 PHOTON FLUX (ARBITRARY UNITS) IN SEVERAL GAMMA-RAY LINES FROM VARIOUS SAMPLES COLLECTED AT OPERATION TEAPOT

The lines are assigned to fission product activities and to induced activities.

Sample No.	Shot	Day	Hours After TZ	Dist. from GZ	Fission Product Lines						Induced Activity Lines Mn^{56} / Na^{24}				
					105	220	280	500	650	750	845	1770	1380	2760	500*
1-1	1	2/18	4.7	Close					0.00	0.00	0.48	0.18	1.31	1.35	0.21
									±0.04	±0.04	±0.08	±0.10	±0.09	±0.0	±0.06
1-2	1	"	8.5	"			0.00		0.00	0.00	2.71	1.11	3.47	3.20	0.89
							±0.13		±0.20	±0.20	±0.25	±0.35	±0.30	±0.30	±0.20
1-2	1	2/19	20.7	"		0.00	0.00		0.00	0.00	0.00	0.00	1.44	1.50	0.15
						±0.02	±0.03		±0.04	±0.04	±0.05	±0.07	±0.15	±0.15	±0.04
3-2	3		9.0	"	6.00	1.60	2.00	4.38	7.55	9.46			2.54	0.74	
					±0.30	±0.16	±0.20	±0.44	±0.75	±0.95			±0.26	±0.07	
3-2	3		27.0	"	5.10	1.20	1.60	1.20	2.37	3.28			0.32	0.33	
					±0.26	±0.12	±0.16	±0.12	±0.24	±0.33			±0.03	±0.03	
4-1	4	3/7	7.3	2400	1.90	0.79	1.22	1.87	4.96	4.57	1.93	0.71	6.19	0.00?	
				yds.	±0.20	±0.20	±0.25	±0.40	±0.40	±0.40	±0.50	±0.40	±0.30	±0.40	
4-1	4	3/8	27.0	"	0.78	0.32	0.62	1.34	2.64	3.42	0.00	0.00	0.00?	0.00?	
					±0.20	±0.15	±0.20	±0.30	±0.40	±0.40	±0.50	±0.10	±0.15	±0.15	
4-3	4	3/8	29.0	600	2.80	2.24	2.91	4.50	5.25	5.40	0.00	0.00	11.75	9.41	
				yds.	±0.50	±0.45	±0.50	±0.80	±0.50	±0.80	±1.00	±0.70	±0.60	±0.90	
7-1	7	3/24	8.5		2.80	1.06	1.01	1.13	0.90	1.07	0.00	0.00	0.00	0.00	
					±0.20	±0.10	±0.13	±0.20	±0.10	±0.10	±0.08	±0.04	±0.06	±0.06	

* Unknown Source.

TABLE 4.2 QUANTITY OF Na^{24} AND Mn^{56} IN EACH SOIL SAMPLE

	A		B		C
Sample No.	Number of Radioactive Mn^{56} Atoms per gram Mn (.854 Mev) $\times 10^{14}$	(% Error)	Number of Radioactive Na^{24} Atoms per gram Na (1.36 Mev) $\times 10^{14}$	(% Error)	Ratio of Radioactive Mn^{56} to Na^{24} in Each Sample
11	12.327	5.91	4.045	5.66	3.05
12a	21.585	5.90	.580	6.41	37.2
12b	21.899	5.90	.643	6.32	34.05
13	5.848	5.95	.640	6.53	9.14
14	.677	6.29	.136	8.17	4.96
15	4.630	5.95	5.114	5.58	.91
16	2.728	5.96	1.166	5.91	2.35
17	4.527	5.94	.793	6.16	5.71
18	5.473	5.94	17.316	5.53	0.32
19	6.518	5.94	24.682	5.50	0.26
20	.856	6.10	13.614	5.52	0.063
21a	4.702	6.00	1.318	6.02	3.56
21b	4.673	6.00	1.328	6.03	3.52
21 later	4.799	5.99	1.370	5.68	3.50
22a	6.770	5.92	.494	6.42	13.70
22b	6.533	5.92	.558	6.33	11.70
22 later	6.654	5.93	.176	6.47	37.74
23	1.936	6.02	.218	8.22	8.86
24	.255	6.65	.061	10.76	4.18
25	1.628	6.00	1.852	5.78	0.88
26	.937	6.16	.356	6.79	2.63
27	1.219	6.07	.247	7.69	4.91
27 later	1.300	5.99	.271	5.82	4.79
28	1.893	5.99	5.192	5.61	0.36
28 later	1.866	6.35	5.400	5.59	0.34
29	1.871	6.06	8.860	5.55	0.21
30	.233	6.57	4.954	5.59	0.047
31	1.031	6.05	.274	7.17	3.75
32	1.469	6.05	.091	10.00	16.11
33	.519	7.01	.086	11.77	6.05
34	.057	9.57	.016	19.20	3.67
35	.437	6.56	.479	6.61	0.91
36	.258	6.76	.112	9.15	2.30
37	.432	6.71	.072	10.81	5.97
38	.451	6.76	1.409	6.09	0.32
39	.465	6.38	1.919	5.74	0.24
40	.057	9.83	1.128	6.15	0.05
41	.264	7.07	.089	10.66	2.95
42	.494	6.58	.038	15.56	13.08
43	.144	7.88	.033	16.68	4.41
44	-	-	-	-	-
45	.129	7.29	.148	8.23	0.87
46	.073	8.36	.047	12.38	1.56
47	.086	8.38	.054	12.68	1.61
48	.124	7.39	.387	7.01	0.32
49	.162	6.86	.613	6.26	0.26
50	.033	13.96	.334	7.03	0.099

CONFIDENTIAL

Table 4.3 compares the measured ratio of Mn^{56} to Na^{24} with the expected ratio using the observed ratios of manganese and sodium in the soil types as determined by the NRDL and Smith-Emery soil chemical analyses. The measured ratio of Mn^{56} to Na^{24} has been determined from the four samples of that type using a weighting factor inversely proportional to the percent error associated with the individual samples. Calculations of expected Mn^{56} and Na^{24} have been made from the soil chemical analyses using the

TABLE 4.3 COMPARISON OF MEASURED Mn TO Na RATIO TO THAT EXPECTED FROM CHEMICAL ANALYSES

Soil Type	Measured Ratio of Mn to Na	Ratio of Mn to Na from Analysis by		Ratio of Mn to Na Expected from Analysis	
		NRDL	Smith-Emery	NRDL	Smith-Emery
0	0.065	0.0063	0.0147	0.063	0.147
1	3.32	0.321	0.595	3.21	5.96
2	21.46	3.503	4.034	35.07	40.40
3	7.12	0.133	1.662	1.33	16.64
4	4.27	0.154	2.293	1.54	22.96
5	0.89	0.0853	0.139	0.854	1.39
6	2.21	0.094	0.189	0.94	1.89
7	4.53	0.444	0.985	4.45	9.86
8	0.32	0.035	0.036	0.35	0.36
9	0.24	0.024	0.031	0.24	0.31

assumption that all activation is produced from (n,γ) reactions in the thermal energy region. For sodium, the thermal neutron cross section used was 0.56 $\pm$0.3 barns, and for manganese, 13.4 $\pm$0.3 barns (Reference 17).

4.3 INCIDENT NEUTRON RADIATIONS

Provided certain assumptions are accepted, it is possible to calculate from the information in Tables 4.2 and 4.3 the incident thermal neutron flux at each of the four sample station locations. Of primary importance is the assumption that all Na^{24} and Mn^{56} activity was produced from Na^{23} and Mn^{55}, respectively, by an (n,γ) process. This is not necessarily true, since it is also possible to produce these radioisotopes by an (n,p) reaction on Mg^{24} and Fe^{56}, respectively, and by an (n,α) reaction on Al^{27}. However, all these reactions have thresholds in excess of 3 Mev. Since neutron flux measurements show (Reference 18) a large predominance in the thermal region, the assumption that all Na^{24} and Mn^{56} is produced by a thermal neutron reaction does not appear unreasonable.

The measured thermal neutron flux was measured (Reference 18) at each of the four sample locations by gold foil detectors. It will be noted that the average neutron flux at both 50 yards and 150 yards from ground zero are consistently lower using the sodium and manganese data

CONFIDENTIAL

TABLE 6.4 THERMAL NEUTRON FLUX AT EACH STATION CALCULATED FROM MEASURED ACTIVITY OF Na^{24} AND Mn^{56} SAMPLES AND NEAL CHEMICAL ANALYSIS

Sample No.	From Na^{24} Activity $\times 10^{14}$	Error in Percent	From Mn^{56} Activity $\times 10^{14}$	Error in Percent
	50 YARD STATION			
11	5.41	7.79	5.14	6.32
12a	6.59	8.23	7.00	6.31
12b	7.31	8.16	7.10	6.30
13	1.98	8.44	13.62	6.35
14	2.27	9.77	7.48	6.66
15	3.49	7.72	4.82	6.35
16	2.26	7.97	7.06	6.36
17	6.76	8.15	8.69	6.34
18	7.82	7.69	7.00	6.35
19	5.18	7.67	5.73	6.34
20	6.19	7.68	6.17	6.49

Thermal Neutron Flux (weighted average) from Na^{24} data---5.65 x 10^{14}.
Thermal Neutron Flux (weighted average) from Mn^{56} data---6.58 x 10^{14}.
Thermal Neutron Flux as determined with gold detectors---8.9 x 10^{14}.

	150 YARD STATION			
21a	1.76	8.05	1.96	6.39
21b	1.77	8.06	1.95	6.40
21 later	1.83	7.81	1.99	6.39
22a	5.61	8.25	2.19	6.32
22b	6.34	8.18	2.118	6.33
22 later	2.00	25.76	2.16	6.62
23	0.68	9.78	4.51	6.62
24	1.04	12.18	2.82	6.77
25	1.64	7.87	1.69	6.40
26	0.87	8.64	2.41	6.55
27	2.10	7.38	2.33	6.46
27 later	2.11	7.83	2.47	6.39
28	2.34	7.75	2.42	6.39
28 later	2.44	7.74	2.39	6.73
29	1.86	7.71	1.64	6.45
30	2.25	7.73	1.68	6.93

Thermal Neutron Flux (weighted average) from Na^{24} data---1.96 x 10^{14}.
Thermal Neutron Flux (weighted average) from Mn^{56} data---2.15 x 10^{14}.
Thermal Neutron Flux as determined with gold detectors---2.3 x 10^{14}.

	250 YARD STATION			
31	0.36	8.94	0.43	6.69
32	1.04	11.32	0.48	6.44
33	0.26	12.44	1.21	7.36
34	0.26	14.74	0.63	9.4
35	0.42	8.53	0.65	6.5
36	0.27	10.56	0.66	7.12
37	0.62	12.03	0.83	6.88
38	0.64	8.10	0.92	7.12
39	0.40	7.04	0.61	6.76
40	0.51	8.15	0.61	6.79

Thermal Neutron Flux (weighted average) from Na^{24} data---0.405 x 10^{14}.
Thermal Neutron Flux (weighted average) from Mn^{56} data---0.52 x 10^{14}.
Thermal Neutron Flux as determined with gold detectors---0.46 x 10^{14}.

	350 YARD STATION			
41	0.12	11.42	0.11	7.61
42	0.43	16.38	0.16	6.96
43	0.12	17.50	0.33	8.18
44	---	---	---	---
45	0.13	9.80	0.13	7.62
46	0.11	23.40	0.17	11.76
47	0.08	13.74	0.16	9.67
48	0.17	9.61	0.16	7.72
49	0.1	8.23	0.14	7.21
50	0.15	9.82	0.20	10.38

Sample No.	From Na^{24} Activity $\times 10^{14}$	Error in Percent	From Mn^{56} Activity $\times 10^{14}$	Error in Percent

Thermal Neutron Flux (weighted average) from Na^{24} data---0.14 x 10^{14}.
Thermal Neutron Flux (weighted average) from Mn^{56} data---0.13 x 10^{14}.
Thermal Neutron Flux as determined with gold detectors---0.14 x 10^{14}.

* M. Cowan, Sandia Corporation, private communication.

CONFIDENTIAL

than was obtained using the gold data. This is somewhat inconsistent with the idea that Na^{24} and Mn^{56} should have been obtained from both thermal and fast neutron reactions. If any discrepancy were noted, it would have been expected to be the reverse of what was observed.

For the neutron-flux calculations presented in Table 4.4, the NRDL quantitative chemical analyses were used for the sample content of sodium and manganese. Some discrepancies will be noted if the Smith-Emery analyses are used. The neutron fluxes at the 50-yard and 150-yard positions are plotted in Figure 4.1 for each sample using both NRDL chemical analyses (Plot A) and the Smith-Emery analyses (Plot B). Note the inversion of the sodium and manganese average neutron flux values between the two analyses. This shift is attributed directly to the soil composition as defined by the two chemical analyses.

Another way of plotting the data is done in Figures 4.2 and 4.3. Using the gold neutron flux values, effective neutron activation cross sections have been determined for each sample. Figure 4.2 shows the results for sodium and Figure 4.3 for manganese. Note that for many samples the cross section is less than the thermal neutron activation cross section, which, as indicated before, is not reasonable. However, in all cases, the value of the cross section for each individual sample is relatively close to the thermal neutron activation cross section, which strengthens the initial assumption that use of the thermal neutron cross section alone is a reasonably valid assumption.

4.4 UNIFORMITY OF SOILS

In discussions with the Soil Conservation Service, emphasis was placed on the fact that these samples, taken at single points, are not representative enough of any one of the individual soils for a specific application of these results. As an example, the fact was emphasized that in the Nevada Test Site area, the salt content of the soil concentrates by a factor of at least 2 directly beneath the desert vegetation. Therefore, the activation per gram of soil taken from an open, unvegetated area will be lower than the same soil surrounded or covered by vegetation. Similarly, numerous soil samples taken from various locations within the Nevada Test Site area have shown, upon analysis, considerable differences in sodium content, approaching a factor of 4.*

The overall reliability of the neutron-flux figures as calculated is open to some question based on the differences in chemical analyses of the soils. The calculation of the number of radioactive atoms at time zero possesses a greater reliability since the soil analysis did not enter these specific calculations.

4.5 DECAY OF SOIL INDUCED ACTIVITIES

The half lives of the two isotopes, Na^{24} and Mn^{56}, found as soil induced activities are 15.0 hours and 2.56 hours, respectively. The half life of the overall soil activity will be dependent upon the relative amounts of these two isotopes present in the soil. For example, Soil 2, Nipe clay, has a large Mn^{56}/Na^{24} ratio; thus, it decays with a half life approaching the 2.56-hour half life of Mn^{56}. Conversely, Sample 0 has a

* M. Coven, Private Communication.

CONFIDENTIAL

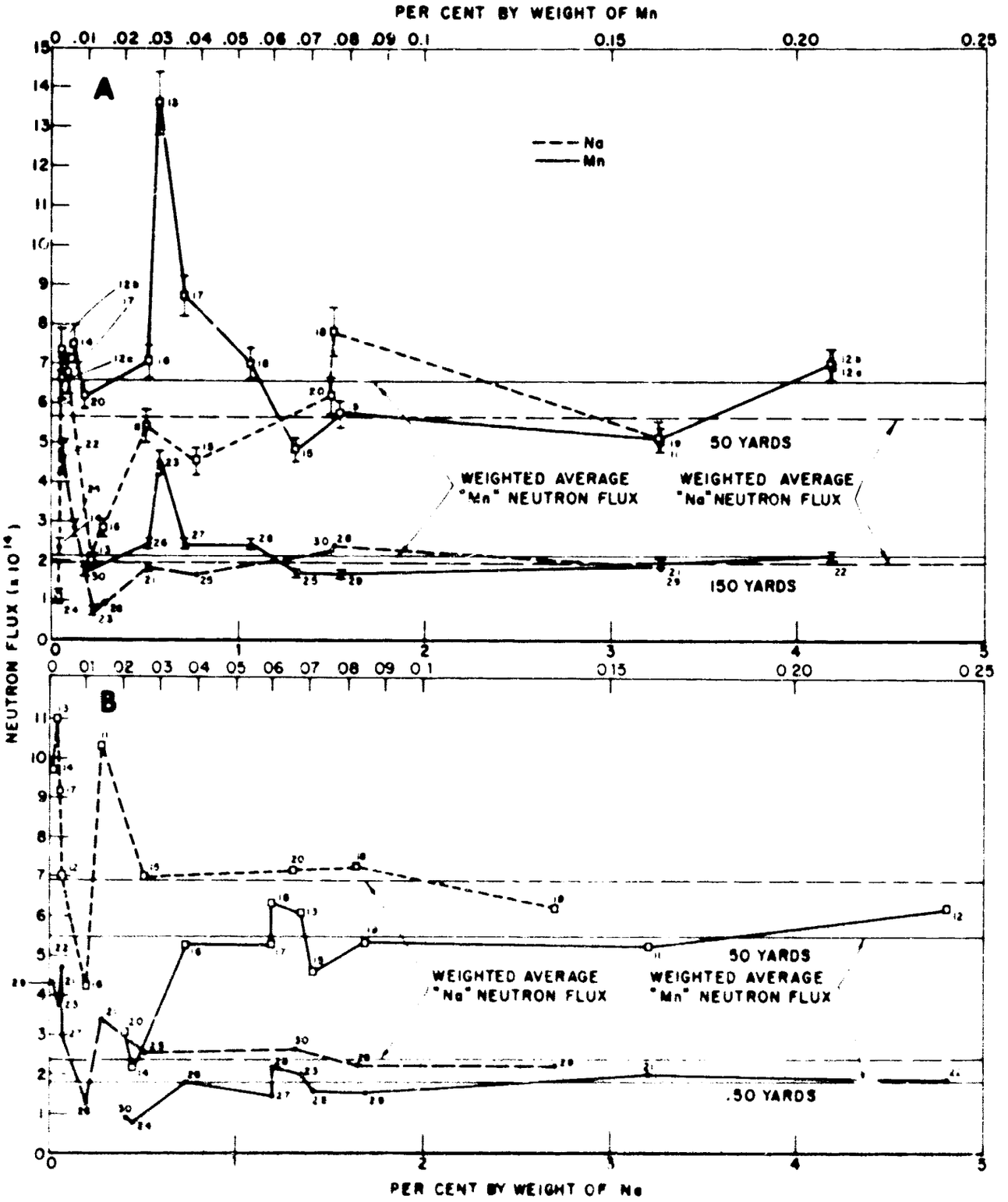

Figure 4.1 Neutron fluxes at 50- and 150-yard positions. A, [illegible] chemical analyses; B, Smith-Emery analyses.

CONFIDENTIAL

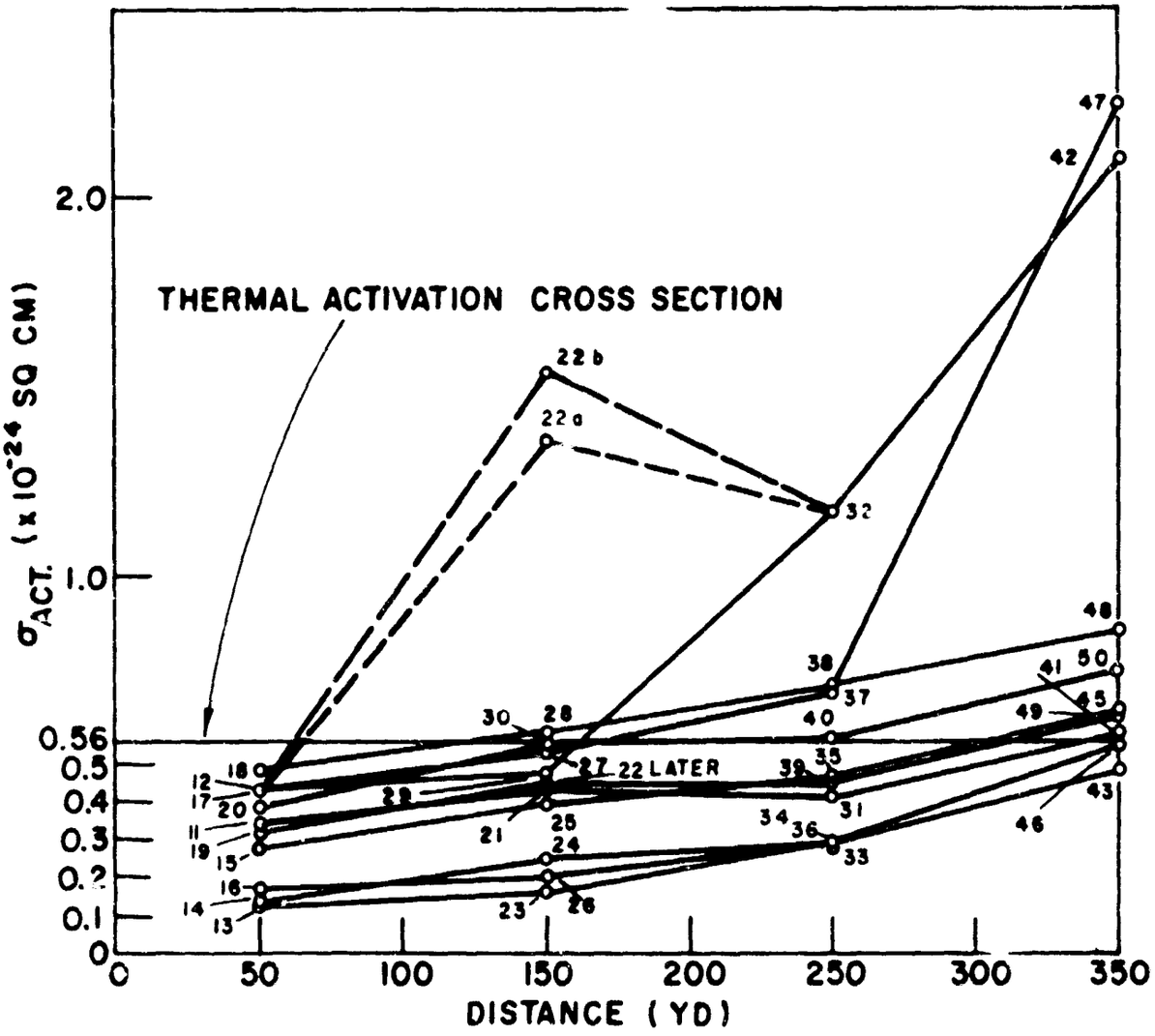

Figure 4.2 Effective neutron-activation cross sections using gold neutron-flux values: sodium.

CONFIDENTIAL

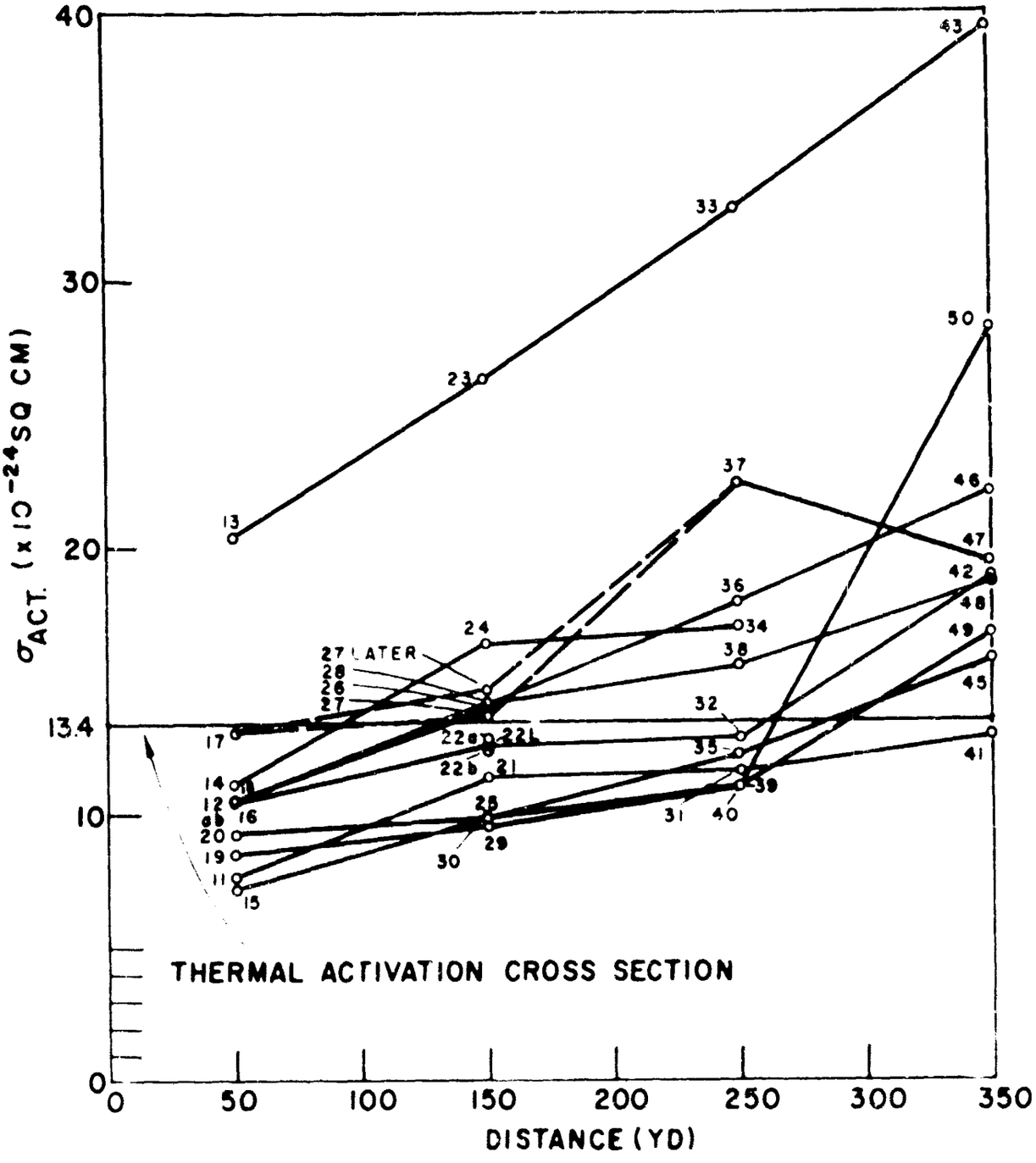

Figure 4.3 Effective neutron-activation cross sections using gold neutron-flux values: manganese.

CONFIDENTIAL

very low ratio, such that its half life approaches the 15.0-hour half life of Na^{24}.

If a mixture of soil induced activities and fission product fallout constitute the radiation field, the observed half life will become strongly dependent upon the induced activity half life within a few hours after detonation, providing the quantity of soil induced activity existing in the mixture is of the same order of magnitude as the quantity of fallout. The gross fission-product half life changes with time, decaying rapidly at early times, leaving the relatively constant decay of the soil induced activities as the major contributor to the activity during a major part of the first day or two after detonation.

4.6 CONCLUSIONS FROM SHOT 5

The relative probability for the production of radioactive isotopes in ten different soils by the neutrons from a specific relatively high neutron-flux experimental device has been found for four different locations relative to ground zero. Only Na^{24} and Mn^{56} activities have definitely been isolated, and it would appear that the induced gamma radiation activities at times greater than 1 hour after detonation from most soil types will be these two radiactive isotopes. What changes would be made because of a different type of device having a different neutron spectrum is unknown. What difference would be made because of differing water content in the soils, with appropriate moderation of the neutrons, is also unknown.

The specific use of these results to calculate the dose rate above a uniform plane of soil, activated by the detonation of a high neutron flux weapon, should be considered only as a tentative answer. Some considerations as to the inaccuracy of this answer are: (1) only four values of activation as a function of distance are known; (2) no information is available concerning the activation as a function of depth below the soil surface; (3) the general gamma-ray field spectra above such a plane is not established with the desired degree of precision necessary for evaluation of dosage; and (4) the relative densities of the various soils and their attenuation of gamma and neutron radiation as a function of density is not established.

4.7 LONG-LIVED ACTIVITIES

Approximately six months after the control pulse height spectra were made, further analyses of a qualitative nature only were performed on soil Samples 11-20, inclusive. The results show some long-lived activity, not of military significance, but in an amount which might possibly have long-term effects. The activities were so weak that quantitative measurements were not possible.

CONFIDENTIAL

Chapter 5
RECOMMENDATIONS

Upon review of this experiment, the following recommendations are made with regard to future work on the subject of induced activities in soils:

1. All samples, which are a mixture of a number of elements, such as soil samples, should be prepared as a uniform, finely-ground, homogeneous material to achieve uniformity for chemical analysis.
2. To obtain information regarding specific areas, representative sampling should be made.
3. The possibility of using pure salts in future exposures should be investigated. The relations to the actual soils could be made mathematically from analysis of chemical content of the soils.
4. Studies should be made on the relative activation as a function of depth below the surface.
5. Further information should be obtained regarding the relative neutron capture cross sections in the soil by elements producing gamma emitters to elements producing non-radioactive isotopes or isotopes decaying only by beta emission. One specific factor to be considered is the effect of water content within the soil.
6. The extension of sampling distance from ground zero is desirable to indicate the effect of neutron spectrum hardening on the capture cross section for the elements present in the soil.
7. Neutron irradiation of selected samples in a reactor or cyclotron beam should be made to evaluate laboratory methods for determining induced activity radiation fields. Field spectral measurements would be required then only as a check of information or to obtain information which could not be obtained in the laboratory.

CONFIDENTIAL

Appendix A

PHYSICAL CHARACTERISTICS OF THE NINE SOIL SERIES SUPPLIED BY THE DEPARTMENT OF ARGICULTURE

A.1 SOIL DESCRIPTIONS

Physical descriptions have been obtained* for the soil series appropriate to nine of the ten soils used in this experiment. While Soil 8 is not described specifically, it does approximately fit the O Spring Series. Some Series Descriptions are listed as tentative and are subject to change by the U. S. Department of Agriculture. Parts of the official descriptions have been deleted for the sake of brevity as not applicable to this experiment.

A.1.1 Soil O. Spring Series. The Spring series includes imperfectly or poorly drained Solonchak soils of the arid Southwest. They are developed on fine-textured valley-filling materials and lake-laid sediments on nearly level land. They are light-colored, calcareous soils, and contain moderate to high concentrations of salts. They occur in southern Nevada where the mean annual precipitation is about 5 inches and the mean annual temperature about 60°F.

a. Soil Profile (Spring clay loam)

1. Light grayish-brown compact calcareous clay loam crust; about an inch thick. The lower part is vesicular and has a pink tinge.

2. Light pinkish-brown friable granular mulch of calcareous heavy clay loam; very plastic when wet; about three inches thick.

b. Variations. Compaction of the subsoil varies considerably, ranging from slightly compact in the fine sandy loam to compact and tough in the clay loam soil types. The lower subsoil is somewhat mottled in the areas of high water table but does not appear to be mottled in most areas. The areas with high concentration of salts have a more pronounced mulch layer than the more nearly self-free areas

A.1.2 Soil 1. Conowingo Series. The Conowingo soils are developed from serpentine in the northern Piedmont Plateau, mainly in Pennsylvania and Maryland. The soils of this series are dominantly shallow but may be very shallow. Where soils are very shallow, areas are locally known as "Barrens." They occur in association with the Chester and Manor soils.

* From U. S. Department of Agriculture, Soil Conservation Service.

CONFIDENTIAL

They are not widely distributed, and their total area seems limited.

a. Soil Profile (Conowingo silt loam, forested)

A_0	1/2-0"	Leafmold consisting of well-decayed plant residues. 0-1" thick.
A_1	0-2"	Light gray (10YR 7/2 - 6/1) silt loam containing some organic matter; weak fine to medium granular structure; very friable; very strongly acid. 1-3" thick.
A_2	2-8"	Light gray (10YR 7/1) silt loam; very friable, non-plastic; very strongly acid. 4-8" thick.

b. Range in Characteristics. Where associated with the Neshaminy, Urbana, Calver, and Aldino series, Conowingo soils grade toward those series. Extensive areas of very shallow soils and some rock outcrops commonly occur in association with typical Conowingo soils. Colors given in the profile description above are for dry conditions. When soil is moist, colors are two or three units of value lower.

A.1.3 Soil 2. Nipe Series. The Nipe series comprise excessively drained dark to dusky red soils (Latosols) derived from serpentine in upland areas of Puerto Rico and Cuba. These soils are easily identified because they stain clothing and skin a "purplish-red" color even when they are dry. The lower parts of buildings constructed on the soil are stained dark red. The clay is the only type in the series, which is not widely distributed nor extensive.

a. Soil Profile (Nipe clay)

0-6"	Very dusky red clay with moderate fine and medium granular structure; soft, friable, very slightly plastic; neutral or slightly acid. 0-8" thick.
6-24"	Dusky red to dark red clay with weak fine granular structure; soft, friable, non-plastic; highly permeable; neutral. 15-30" thick.

b. Range in Characteristics. The darker surface layer is occasionally more than 8 inches thick, but it may be entirely lacking because of erosion. Depth to bedrock is commonly great, ranging from a few to many feet in diameter. Low fertility of the soil is reflected in slow growth of vegetation.

c. Distribution. Western Puerto Rico and eastern Cuba.

A.1.4 Soil 3. Koolau Series. The soil of the Koolau series occurs in wet regions at the upper limit of the areas used for grazing or at the lower limit of present forests. It is at elevations ranging from 400 to 5,000 feet and receives an annual rainfall of 100 to 250 inches. The soil occurs entirely within vegetation zone b_2 on the islands of Kauai, Maui, Molokai, and Oahu.

CONFIDENTIAL

The Koolau soil occupies the driest part of the region occupied by the Hydrol Humic Latosols, but rainfall is extremely high. The profile is characterized by the grayness of the A_1 horizon, the yellowness of the B horizon, and the "smeariness" of the soil material when it is wet. When the soil dries, the clays dehydrate irreversibly and form hard granules. The soil is very highly leached and almost completely depleted of bases. Silica has also been removed, so there are high concentrations of iron and aluminum compounds. Silica-sesquioxide ratios are generally 0.5 or below.

a. Soil Profile (Koolau clay)

A_1	0-9"	Dark gray silty clay; moderately developed course or medium granular structure; friable when moist, firm or hard when dry, smeary when wet; pH 4.0 to 5.0; roots very numerous.
B	9'27"	Yellowish-brown to yellowish-red silty clay; moderately developed medium blocky structure; hard when dry, friable when moist, strongly smeary when wet; pH 4.0 to 5.0; roots present; may be weakly mottled with gray in lower part.

In places the Koolau soil appears to be developing into a soil comparable to those of the Humic Ferruginous Latosol group. The surface layer in these areas is silty and high in bulk density, and on close examination is seen to be made up of fine earth in which are many tiny glistening specks. Under the microscope, these specks are seen to be definite crystals that have been identified in other soils as magnetite, anatase, or ilmenite. An area on the island of Oahu has been included that has a concentration of resistant primary minerals in a kaolinite base. The inclusion of resistant materials is thought to be an exception rather than the rule for the series as a whole.

The soil properties vary somewhat with elevation and with increasing rainfall. At the lower altitude limit, the soils grade into the Humic Latosols; and A_1 horizons are more distinctly granular and browner and the B horizons are more distinctly reddish. Near the upper and wetter limits of the series, the soil assumes some hydromorphic characteristics. The A_1 horizon is less distinctly yellowish and in some places may be weakly mottled with gray in the lower part. The mottling indicates poor aeration. The series as a whole, however, consists of material that is very porous and is easily penetrated by water. This material has high water-holding capacity, and the clays shrink markedly on drying.

A.1.5 Soil 4. Norfolk Series. The Norfolk series include the most prominent of the Yellow Podzolic soils in the Atlantic and Gulf Coastal Plains. These soils have been formed from thick unconsolidated beds consisting chiefly of acid sandy clay loams in which there are layers of sand, sandy loam, and sandy clay. Because of its wide distribution, the Norfolk series is associated with a large number of other soils. It is perhaps most frequently associated with and closely related to the Marlboro, Tifton, Ruston, Gilead, Orangeburg, Lakeland, and Kershaw soils. The Norfolk series may also be associated with a number of other soils such as the

CONFIDENTIAL

Bowie, Blanton, Susquehanna, Bowwell, Cuthbert, and Shubuta series. The Norfolk, Marlboro, and Tifton soils have profiles that are similar morphologically in many respects. Norfolk soils have thicker A horizons, more friable B horizons, and sandier solums than do Marlboro soils. They lack the weakly cemented B horizons and the fine textured C horizon of the Gilead soils. They are lighter colored, less brown, and contain fewer concretions throughout the profile than the Tifton series which also has a more sticky B horizon. Norfolk soils have more uniformly colored lower B horizons and are less fine textured in the C horizon than are Bowie soils. They are much more yellow in the B horizon and perhaps less well-drained on the whole than the Ruston and Orangeburg series which are members of the Red Podzolic group. They have much shallower surface layers of sandy materials than do the Lakeland and Kershaw series. The Norfolk series is one of the most widely distributed and extensive soils in the Atlantic Coastal Plain and in the eastern part of the Gulf Coastal Plain. The series is used for a large variety of crops and is of major agricultural importance.

a. Soil Profile (Norfolk fine sandy loam)

A_1	0-2"	Dark gray[1] to gray nearly loose loamy fine sand or light fine sandy loam with fine weak crumb structure; strongly acid. 1-4" thick.
A_2	2-15"	Pale yellow nearly loose loamy fine sand or very light fine sandy loam; essentially structureless; strongly acid. 8-14" thick.
B_1	15-18"	Yellow to light yellowish-brown very friable fine sandy loam or light fine sandy clay loam with medium weak blocky structure; strongly acid. 2-6" thick.
B_2	18-38"	Yellow to light yellowish-brown friable fine sandy clay loam with medium moderate to weak blocky structure; strongly acid. 14-24" thick.

b. Range in Characteristics. The principal types in the series are sandy loams and loamy sands. Phases are recognized where the thickness of the A horizon exceeds 18 inches but not 30 inches. Where the sandy material is more than 30 inches thick, on the average, the soil is included in the Lakeland series. In cultivated fields the A_1 horizon is mixed with the upper part of the A_2 horizon and loses its identity. The texture of the B_2 horizon is commonly sandy clay loam but it may be a heavy sandy loam or a light sandy clay. Small rounded quartz gravel are present on the surface and throughout the profile in places. There may also be some small rounded iron concretions in the soil, especially where it is associated with the Tifton series.

---

[1] Provisional soil survey color names, 1946, have been used.

CONFIDENTIAL

c. Distribution. North Carolina, South Carolina, Virginia, Georgia, Alabama, Florida, Mississippi, Louisiana, Arkansas, and eastern Texas.

d. Remarks. The deeper sands and loamy sands formerly included in the series are now included chiefly in the Lakeland and Kershaw series. Norfolk series, named for the city in Virginia, is no longer recognized in the original area, Cecil County, Maryland.

A.1.6 Soil 5. Carrington Series. The Carrington series includes zonal Prairie soils developed on Iowan till which has slight to medium plasticity, a heavy loam to sandy clay loam texture, and is leached to 50 or 55 inches. They resemble in color the Tama soils of loessial origin and are distinguished from the Clarion soils, which are developed in glacial till of the Mankato subage of the Wisconsin, in having slightly heavier textured B horizons, a greater depth to free carbonates, and a more compact and plastic underlying till, which was a heavy sandy clay loam texture.

a. Soil Profile (Carrington loam*)

1. Dusky-brown to brownish-black when moist; loose. mellow, fine granular loam; strongly acid. 8-12" thick.

2. Transition layer, ranging from granular, dusky-brown loam or clay loam in the upper part, to brown clay loam in the lower part, strongly acid. 8-10" thick.

3. Dark yellowish-brown heavy loam to clay loam, weakly sub-angular. The material is well oxidized and leached of carbonates; slightly acid.

b. Range in Characteristics. The surface layer varies in thickness and darkness with the degree and shape of slope. A thin covering of loess may have added to the composition of the more silty types. Occasional boulders and gravel are scattered over the surface of these soils and through the soil section.

c. Distribution. Eastern Iowa and Minnesota.

A.1.7 Soil 6. Chester Series. The Chester series are gray-brown Podzolic soils of the northern part of the Piedmont Plateau. The soils are underlain by and developed from the weathered products of gneiss, granite, and schist. They occupy the smoother relief flanked by the more steeply sloping lands with less developed soils of the Manor series. Acid in reaction.

a. Soil Profile (Chester loam)

A_1	0-3"	Pale brown to weak brown loam with considerable organic matter and a shallow covering of leafmold; fine to medium weak crumb structure; strongly acid. 1-3" thick.

* Colors according to Misc. Pub. 425, U.S.D.A.

CONFIDENTIAL

A_2 3-12" Light brown to brownish-yellow loam; mellow and friable. Both of these layers carry a high percentage of silt. In cultivated fields the surface is brownish to gray to light yellowish-brown. Fine weak crumb structure; strongly acid. 6-10" thick.

b. Range in Characteristics. Small areas having brown soils and reddish-brown subsoils are now recognized as Elioak where they occur in sufficient size to delineate; texture ranges from silt loam to slate loam.

c. Distribution. Pennsylvania, Maryland, Virginia, and Delaware.

A.1.8 Soil 7. Houston Black Series. This is a monotype series consisting of Houston Black clay and its several phases, which are black to dark gray granular clayey Rendzinas developed on chalk, marl, or calcareous clay in warm-temperate humid prairies. Where developed on chalk or chalky marl the associated series are Austin and Eddy; where developed on calcareous clays or clayey marls the associated series are Wilson, Hunt, Houston, and Sumter. Houston Black is a darker, less granular, deeper, and less permeable than Austin, the content of clay throughout the solum being greater, and of $CaCO_3$, lower. Houston soils are browner and generally more sloping and less deeply developed than Houston Black clay. The series similar to Houston Black but developed in the Grand Prairie on limestones interbedded with marls is San Saba; the noncalcareous equivalent is Hunt; and the stream terrace analogue is Bell.

a. Soil Profile. (Houston Black clay)

0-18" Very dark gray (black when moist) clay; medium granular; very sticky and plastic when wet; very crumbly when slightly moist; calcareous. 10-20" thick.

16-40" Same as horizon 1 except that it is weakly granular to coarse blocky, lower in organic matter, and contains a few concretions of $CaCO_3$ in lower part. 0-30" thick.

b. Range in Characteristics. Thickness of dark layer is wavy and ranges from 5 to 50 inches in relation to micro-relief; color of horizon 1 ranges from black to dark olive gray and gray (values of 2/ to 5/); where developed over chalk, horizon 2 is dark grayish brown and strongly granular; shallow phases are 15 to 30 inches deep over chalk; gravelly phases have water-worn pebbles of chert and quartzite on the surface; in level phases the lower subsoil is gray.

c. Distribution. Prairies within the Gulf Coastal Plain in eastern central Texas, southern Oklahoma, Alabama and probably Arkansas.

d. Remarks. The soil has an extremely high coefficient of expansion and contraction on wetting and drying and the clay content

CONFIDENTIAL

generally exceeds 60 percent. Crevices 3 to 6 inches wide and extending to a depth of several feet form during extremely dry periods, and puddled material crumbles with one thorough wetting and drying. Prior to 1940, Houston Black clay was regarded as a black clay type of the Houston series but is now of a separate series, Houston Black. Colors are described with provisional Soil Survey color names and refer to dry soil unless stated otherwise.

A.1.9 Soil 9. Niland Series. The Niland soils are azonal soils of the southwestern desert region. They are calcareous, friable, gray, and are derived largely from gravelly alluvial wash over lake-laid sediments. These soils occupy ancient beach lines at the outer margins of the former Salton Sea in California. They occur in southeastern California where the mean annual precipitation is about 3 inches, mean annual temperature about 70°F, winters are mild, and summers very hot. The precipitation occurs mostly in two periods---early autumn and late winter.

a. Soil Profile (Niland Gravelly sand). Light grayish-brown or light brownish-gray calcareous incoherent sand; very low in organic matter; has a quantity of water-worn gravel, consisting principally of granite, chert, quartz, and sandstone ranging from 1/2 to 3 inches in diameter, scattered on the surface, but rarely below a depth of 3 inches; about 8 inches thick.

b. Variations. Chiefly in depth of the alluvial material above the stratified lake-laid sediments and in the texture and color of the stratified layers. These layers are exceedingly variable. In a few places the surface soil has an ashy-gray cast and in some places conglomerate-like gravels cemented with lime occur on the surface.

c. Distribution. Southeastern California.

CONFIDENTIAL

REFERENCES

1. Feld, B. T.; The Neutron; Experimental Nuclear Physics, edited by E. Segre (John Wiley and Sons, Inc., New York, 1953), Vol. II, Pages 208 ff, UNCLASSIFIED.

2. Terrell, J., and Holm, D. M.; Physical Review (to be published); UNCLASSIFIED; see also WASH-191, Page 26, CONFIDENTIAL.

3. Wolfe, R. D.; Program Reports, Gross Weapons Measurements; Vol. 4; Operation Ranger, WT-201, June 1952, SECRET-RD.

4. Shipman, T. L.; Radiological Safety; Operation Buster-Jangle, WT-425, July 1953; SECRET-RD.

5. Gwynn, P. S.; Radiological Safety; Operation Tumbler-Snapper, WT-558, December 1952; SECRET-RD.

6. Collison, T. D.; Radiological Safety; Operation Upshot-Knothole, WT-702, June 1953; CONFIDENTIAL.

7. Capabilities of Atomic Weapons, TM-23-200, Page 67, 1 June 1955; SECRET-RD.

8. Cowan, M., Jr. and Cook, T. B., Jr.; Residual Contamination; SC-3466(TR), 15 February 1955; SECRET.

9. Dike, S. H.; A Note on Induced Contamination from Air Bursts; SC-3616(TR), 27 April 1955; SECRET.

10. Dike, S. H.; The Radiation Hazard of Areas Contaminated by Air Bursts; SC-3626(TR), 4 May 1955; SECRET.

11. Fano, U.; Gamma-Ray Attenuation---Basic Processes; Nucleonics, 11, No. 8, 8-12(1953); UNCLASSIFIED.

12. Bouquet, F. L., Kreger, W. E., Mather, R. L., and Cook, C. S.; Application of a Scintillation Spectrometer to Radioactive Fallout Spectral Analysis; USNRDL-420, 31 August 1953; CONFIDENTIAL.

13. Cook, C. S., Johnson, R. F., Mather, R. L., Tomnovec, F. M., and Webb, L. A.; Gamma-Ray Spectral Measurements of Fallout Samples from Operation Castle; USNRDL-TR-32; January 1955; CONFIDENTIAL-RD.

14. M. J. Berger and J. A. Doggett; Response of NaI(Tl) Scintillation Spectrometers; Review of Scientific Instruments, 27, 269 (1956) and Journal of Research of NBS 56, 355 (1956); UNCLASSIFIED.

15. Foote, R. S., and Koch, H. W.; Scintillation Spectrometers for Measuring the Total Energy of X-Ray Photons; Review of Scientific Instruments 25, 736 (1954); UNCLASSIFIED.

16. Griffiths, G. M.; The Pulse Height Distribution from a Sodium Iodide Single Crystal Scintillation Counter and the Measurements of Gamma-Ray Fluxes; Canadian Journal of Physics 33, 209 (1955) UNCLASSIFIED.

17. Hughes, D. J., and Harvey, J. A.; Neutron Cross Sections; BNL-325, July 1, 1955; UNCLASSIFIED.

18. Harris, P. S., and others; Physical Measurements of Neutron and Gamma Radiation Dose from High Neutron Yield Weapons and Correlation of Dose with Biological Effect; ITR-1167, Project 39.7, Operation Teapot; SECRET-RD.